(1)
(4)



EARTH SCIENCES
A TELEDYNE COMPANY

# FINAL REPORT
# QUADRUPOLE MASS SPECTROMETER
# ES-4103
July 1969

Contract No. NASW-1736

Prepared for

NASA Headquarters
Code SL, Attn. Mr. Don Easter
Washington, D. C. 20546

Prepared by

W. M. Brubaker

W. M. Brubaker*, Project Manager

Earth Sciences
A Teledyne Company
171 North Santa Anita Avenue
Pasadena, California 91106

*Present Address: Analog Technology Corporation
3410 E. Foothill Boulevard
Pasadena, California 91107

## ABSTRACT

In anticipation of building a tandem quadrupole mass analyzer, computations were made of the influence of the transients given ions at the junction of mass filters operating at the same frequency, but at different resolving powers. Data compiled show that the addition of a mass filter operating at a low resolving power before one operating at a higher resolving power negligibly affects the amplitudes of the trajectories in the latter unit.

Theoretical and experimental studies are made of the operation of a quadrupole mass spectrometer in the presence of a high background pressure of hydrogen. The mass filter was found to be amazingly tolerant of the high pressure. When ions from a thermal source are introduced, the resolving power remains unaltered at pressures of $10^{-2}$ torr. Transmission efficiency of these thermal ions starts to decrease at a pressure of $10^{-3}$ and is down to about 20 percent at $10^{-2}$. When an electron bombardment ion source is used, the space charge of the positive ions degrades the resolving power attained at a given transmission efficiency at pressures above $10^{-5}$ torr. Comparisons of wide mass range spectra made in the conventional and in the delayed dc ramp modes illustrate the predicted discrimination against ions of high mass. The discrimination results from the longer time required for ions of heavy mass to traverse the entrance fringe fields where the y-trajectory is highly unstable.

## CONTENTS

CONTENTS Continued

## INTRODUCTION

As the items of the original Work Statement (page 2) indicate, this project was designed to study the performance of a tandem quadrupole with one straight section and one curved section. It is anticipated that an instrument of this configuration would exhibit superior performance capabilities. Engineering drawings for the curved section were made, but before fabrication was begun, the emphasis shifted from fundamental studies to the practical problems associated with the use of a quadrupole mass spectrometer in conjunction with a gas chromatograph. The Amended Work Statement (page 3) reflects this change in emphasis.

## WORK STATEMENT

Provide personnel and equipment and perform the following tasks in accordance with Earth Sciences Proposal ESD-1366 dated November 10, 1967:

A. Conduct a computer investigation of the transient given the ions at the junction of the straight and curved portions of the quadrupole structures.

B. Design, fabricate, and assemble a quadrupole mass filter with a curved and a straight portion. Each portion will have insulated segments at the appropriate places on each rod.

C. Using the apparatus described in B, study the photon-induced signal at the output of the secondary electron multiplier and compare the results with those obtained with a conventional, straight quadrupole of similar dimensions.

D. Using the apparatus described in B, observe the sensitivity versus resolving power and compare the results with those obtained using a straight quadrupole of similar dimensions.

E. Using the apparatus described in B, study the vulnerability of the instrument when analyzing one gas to the presence of a second gas at high concentration. Compare the results with those obtained with a quadrupole of similar dimensions, but with the straight portion only.

F. Repeat items C, D, and E with the source and detector interchanged.

G. Using the relation of sensitivity to resolving power data as a criterion, explore the number, length, and excitation pattern of the segments most appropriate for obtaining optimum entrance conditions.

## AMENDED WORK STATEMENT

Item 1. Conduct a computer investigation of the transient given the ions at the junction of the straight and curved portions of the quadrupole structures.

Item 2. Design, fabricate, and assemble a quadrupole mass filter with a curved and a straight portion. Each portion will have insulated segments at the appropriate places on each rod.

Item 3. Extend mass scan range capability, giving particular attention to factors which influence mass discrimination.

Item 4. Perform laboratory experiments designed to explore the parameters which influence mass discrimination.

Item 5. Perform experiments designed to demonstrate the capability of the quadrupole to make quantitative analyses over a wide mass range.

Item 6. Using the hyperbolic rod quadrupole developed under Contract NASW-1298, study the vulnerability of the instrument when analyzing one gas to the presence of a second gas at high concentration.

## COMPUTER STUDIES OF TRAJECTORIES THROUGH TRANSITION REGION AT JUNCTION OF SECTIONS OF TANDEM QUADRUPOLE

In the operation of the tandem quadrupole (with one curved and one straight section), it is anticipated that the resolving power of the first section will be adjusted to a lower value than that of the second section. This change in the resolving power, which is accomplished by applying different potentials to the two sections, introduces a transient in the motion of an ion as it traverses the region of changing fields. The purpose of the computer study is to explore the magnitude of this transient and to observe its influence on the ionic trajectory. It is realized that the effect of this transient depends on the time the ion spends in the transition region, as well as on the phase of the applied ac potential when the ion enters the changing fields.

### COMPUTER STUDIES

The computer study explores the effect of the transient on the trajectory of an ion as a function of two variables: (1) the phase of the ac excitation voltage when the ion enters the transition region and (2) the position of the ion when it enters the transition region. To accomplish this, the actual trajectories of the ions in both the x and y directions are plotted. For simplicity in the calculations, the two quadrupoles are assumed to be straight; that is, no consideration is given to the perturbation introduced by curving one of the sections.

For purposes of calculation, the electric field in the region of the adjoining quadrupoles is assumed to increase in

a linear ramp from the field of the low-resolving power section to the field of the high-resolving power section. On the computer, this change takes the form of a linear increase in $a$ and $q$ along a path between two working points on the stability diagram corresponding to resolving powers of approximately 50 and 130. The change takes place over a period equal to two cycles of the ac rod voltage and is initiated at various points on the low-resolving power trajectory corresponding to different phases of both the ac rod voltage and the trajectory envelope.

Trajectories were first obtained for ions in a normal quadrupole field. The plots were computed for ions entering the field on the axis with equal components of radial velocity in both the x and y directions. The trajectories were obtained for both of the working points on the stability diagram mentioned previously. These working points were chosen to fall on the line $\beta_x + \beta_y = 1$ so that the amplitudes and periods of the x and y trajectory envelopes would be similar.

The envelopes of the trajectories for the two resolving powers are shown in Figure 1. Both $A_2/A_1$ and $t_2/t_1$ are nearly equivalent to the square root of the ratio of the resolving powers, as predicted by theory.

Trajectories were then obtained for the tandem case, using the two cycle ramp described above. A pair of sample trajectories, showing the changes in the amplitudes and periods for x and y is shown in Figure 2.

From a number of such calculations which have been made, it can be concluded that:

1. The period of the trajectory envelope in the second quadrupole is characteristic of its fields and is completely independent of the manner in which the ions are introduced into it.

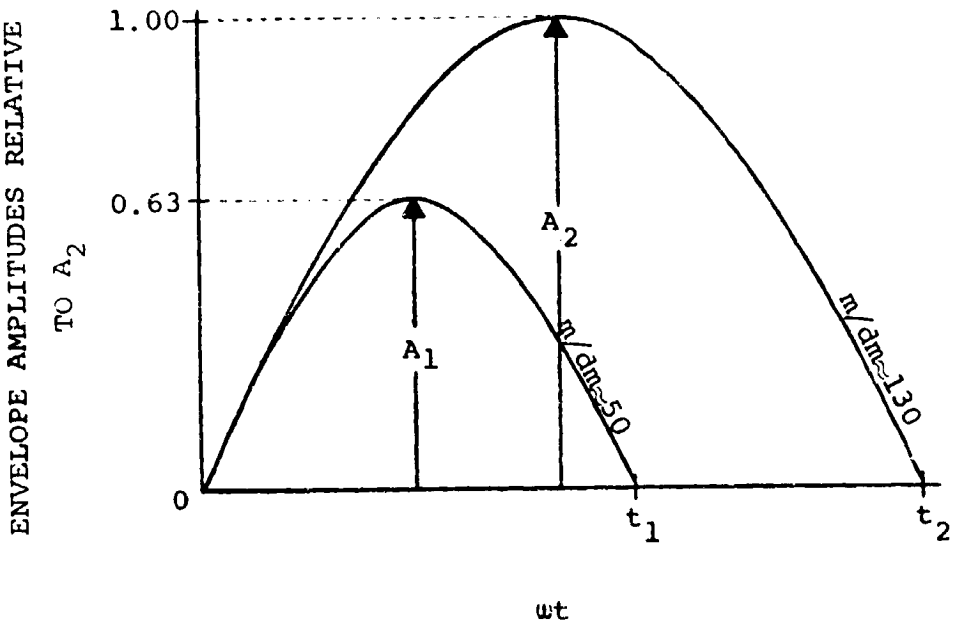


Figure 1. Envelopes of Trajectories at Two Resolving Powers

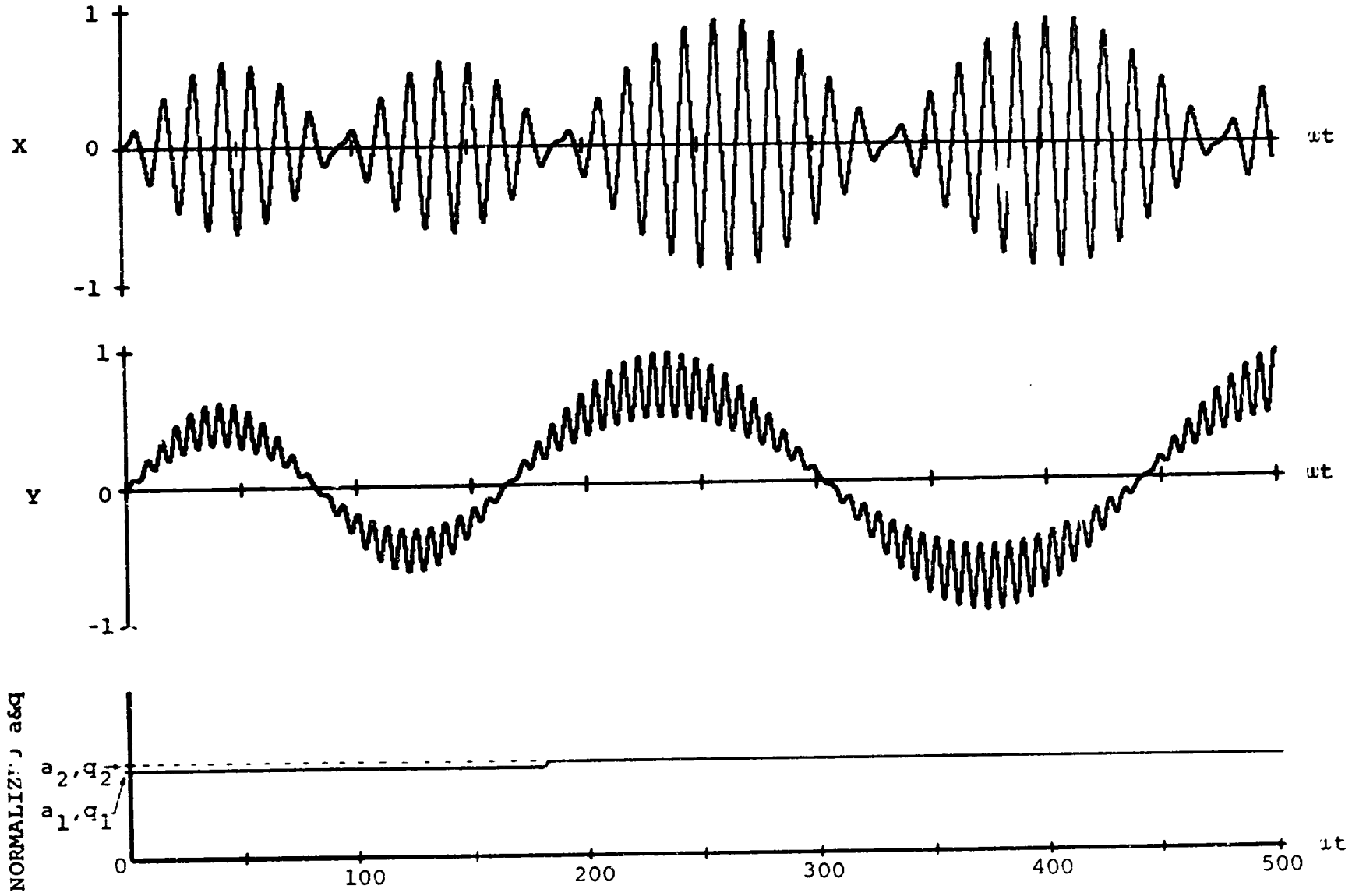


Figure 2. Trajectories of Ions Through Tandem Quadrupoles

2. The amplitude of the trajectory envelope in the second quadrupole is independent of the phase of the ac rod potential at the onset of the transition region.

3. The amplitude of the trajectory in the second quadrupole is influenced by the phase of the trajectory envelope at the onset of the transition region.

   a. If the amplitude of the trajectory envelope is very small at the junction, the amplitude in the second quadrupole is the same as though the ion had entered the high resolving power region directly.

   b. If the amplitude of the trajectory at the junction is near its maximum, then the amplitude in the second quadrupole is less than in a. above.

   c. Between these two extremes, the amplitude varies sinusoidally as shown in Figure 3.

## CONCLUSIONS

The computer studies indicate that the transients given ions as they traverse the junction of the two sections of the tandem quadrupole are of little importance. The net effect of placing a quadrupole adjusted to low resolving power in front of a quadrupole adjusted to high resolving power is to decrease the trajectory amplitudes in the higher resolving power unit. This is a desired condition, because it increases the transmission probability for the ions.

The computations encourage the development of a tandem quadrupole.

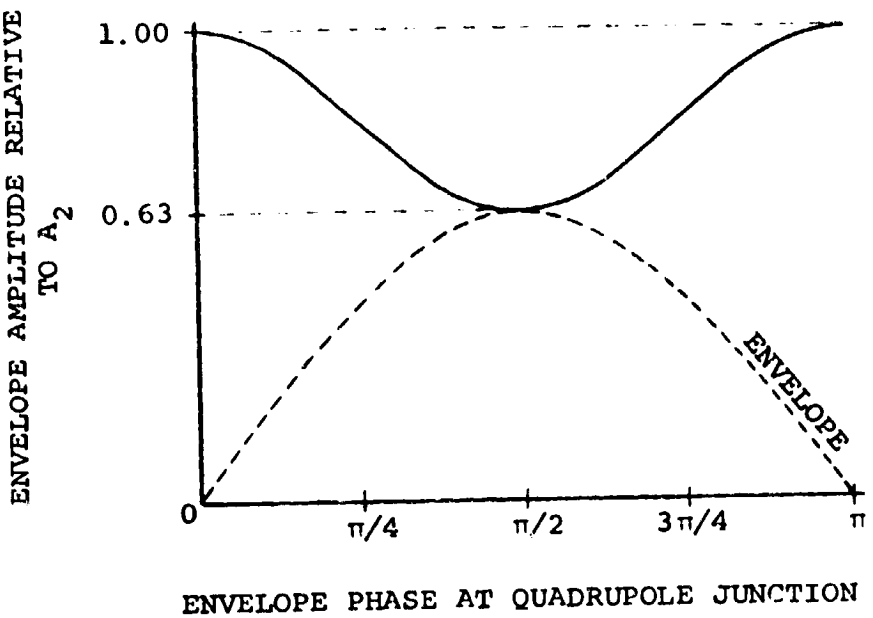


Figure 3. Amplitude of Trajectories in High Resolving Power Unit as a Function of the Phase of Trajectory Envelope at the Junction of the Quadrupoles

## TANDEM QUADRUPOLE

The contemplated quadrupole consists of two sections, one curved and one straight. This tandem arrangement has several distinct advantages. First, the use of a curved guide for the ions separates them from the photon beam which emanates from the ion source. If the photon beam is allowed to impinge upon the detector, there results a very objectionable "background" which masks low level signals associated with trace components of the gas sample being analyzed. Second, the tandem sections form two separate mass analyzers in series. It is anticipated that the first section will be used as an analyzer of low resolving power relative to that of the second. In the case of magnetic analyzers, this scheme has been found to enhance the ability of the device to respond to a small peak which is adjacent to a much larger peak. Similar results are anticipated with the tandem quadrupoles. This is of particular importance for the mass analyzer used in conjunction with a gas chromatograph.

A tandem quadrupole assembly has been designed, and engineering drawings are completed. It consists of a curved section and a straight section, as shown in Figures 4 and 5. The straight section has rods of hyperbolic cross section, each of which has an insulated segment at one end. This is the quadrupole which was used in the experiments performed under Contract NASW-1298. The curved section has round rods and is designed to attach to the existing straight section to form the tandem unit. The newly designed portion includes a short, straight, segmented rod portion which can be placed at either end of the tandem assembly. This portion carries

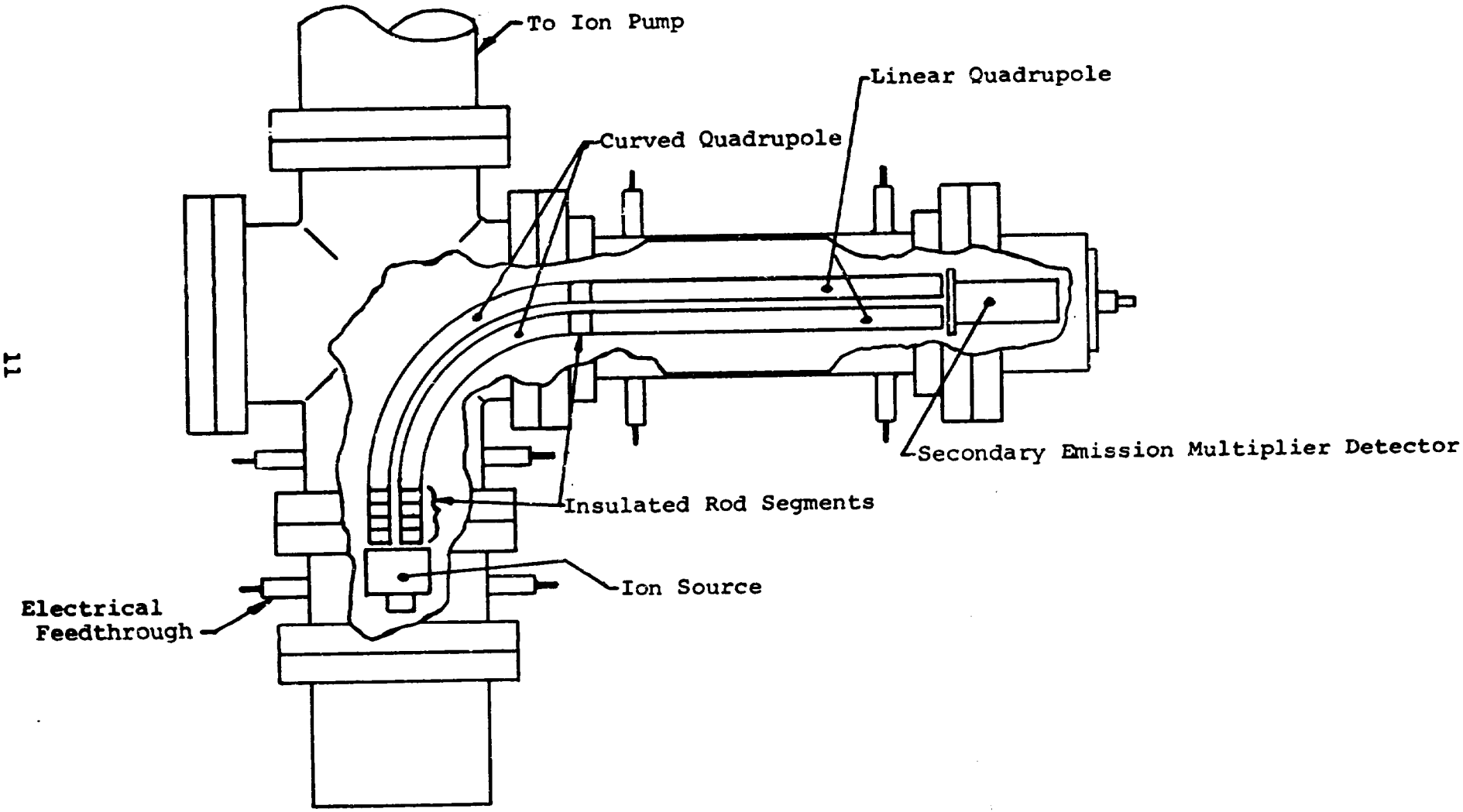


Figure 4. Tandem Quadrupole with Source Adjacent to Curved Section

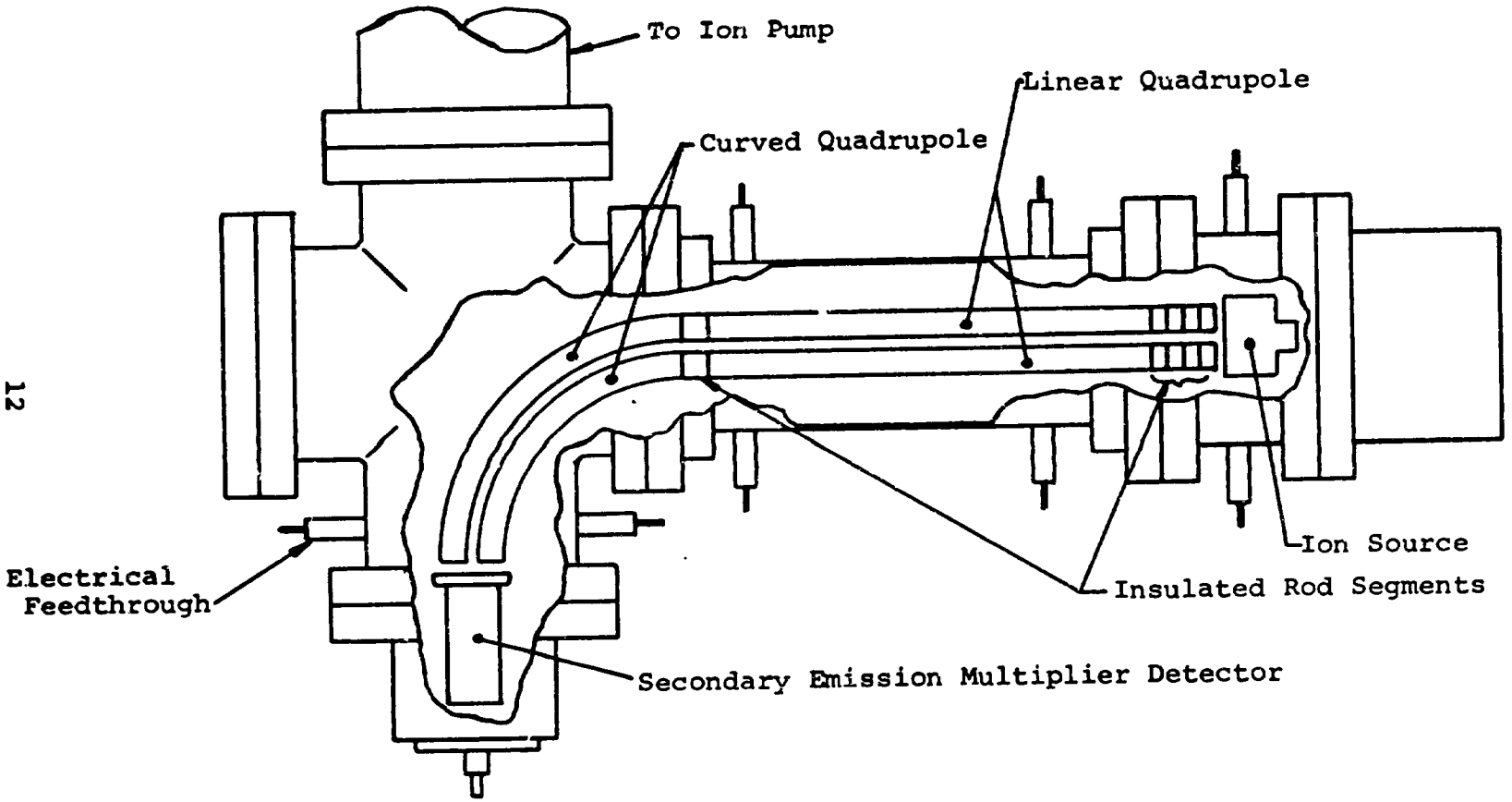


Figure 5. Tandem Quadrupole with Source Adjacent to Straight Section

four segments for each of the four rods. Individually, these segments are shorter than the ones used in the previous tests (NASW-1298). However, external connections are provided for each pair of opposing segments. Thus, it is possible to combine them in any desired manner, changing their effective lengths. The design is such that the straight section can be turned end-for-end, placing the insulated segments at the chosen places. This flexibility leads to the various configurations shown in Figures 6 and 7.

Figure 6 depicts the source adjacent to the curved section, the detector adjacent to the straight. In Figure 7 the source and detector are interchanged. The three variants in each of the above cases indicate the different manners in which the apparatus can be assembled to locate the insulated segments at chosen positions in the tandem assembly. This flexibility is in accord with Item 2 of the Amended Work Statement which reads, "Each portion (of the tandem assembly) will have insulated segments at the appropriate places on each rod."

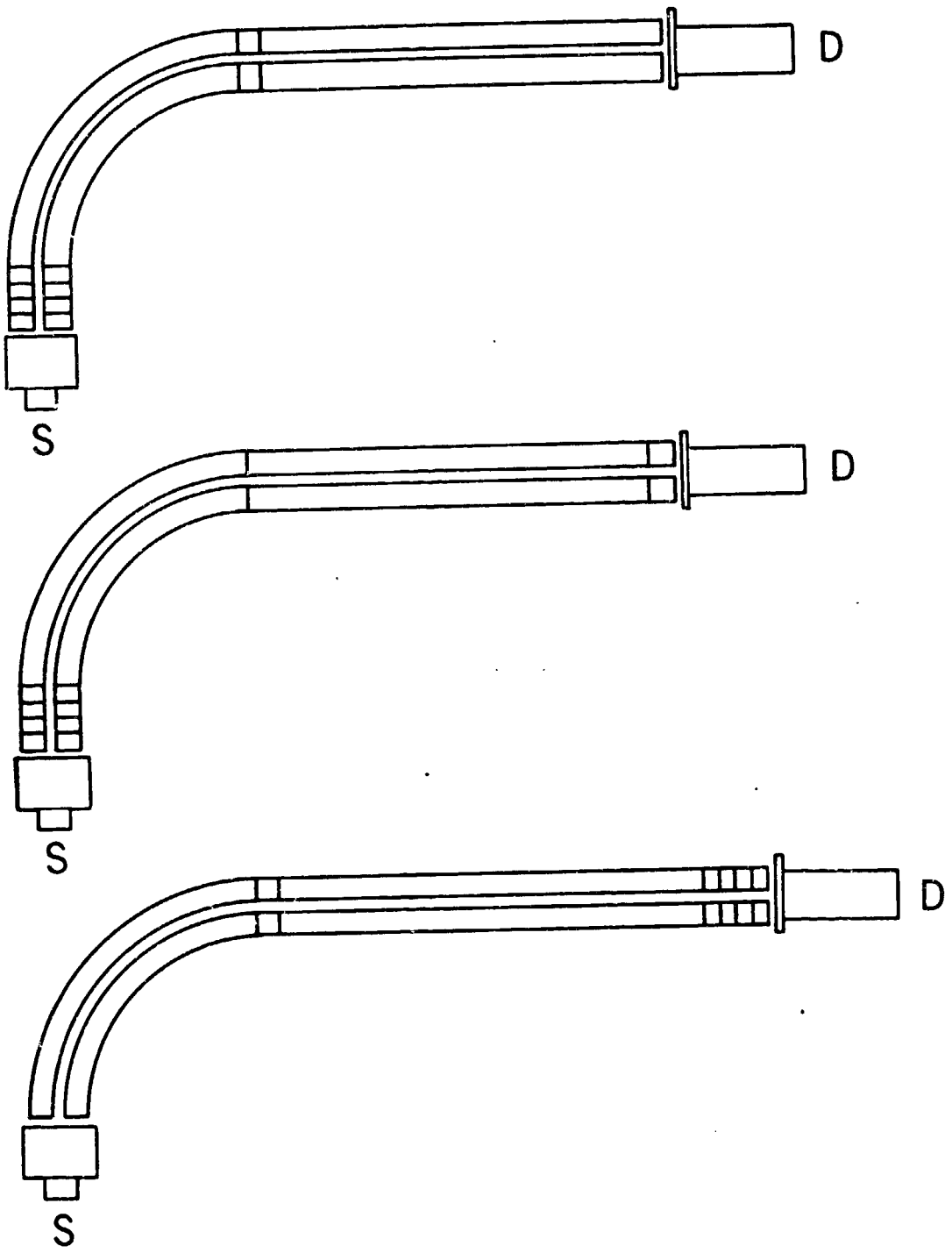


Figure 6. Various Arrangements of Segments With Source Adjacent to Curved Section

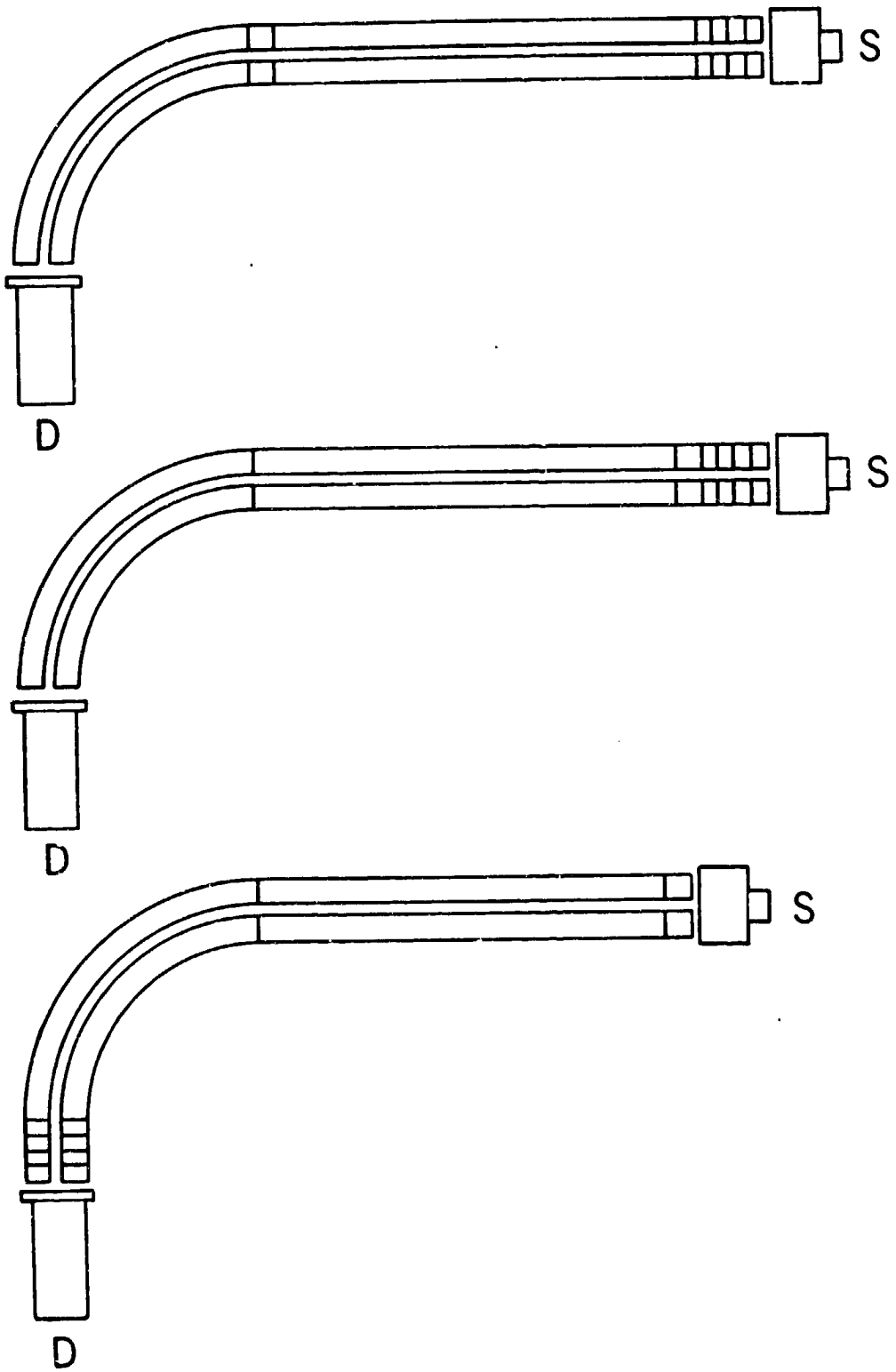


Figure 7. Various Arrangements of Segments With Source Adjacent to Straight Section

## EXPERIMENTS WITH THE 10-INCH HYPERBOLIC QUADRUPOLE

The amended work statement mentions the two areas of primary concern in the experiments. These areas are: (1) mass discrimination in quadrupole mass spectrometers, and (2) operation of the quadrupole at high pressures. A few changes in the apparatus are required for these experiments.

### APPARATUS

#### Mechanical

The apparatus used for these experiments is essentially the same as that used in the performance of Contract NASW-1298, "A Study of the Introduction of Ions into the Region of Strong Fields within a Quadrupole Mass Spectrometer." It is shown in block form in Figure 8. The effective pumping speed has been reduced to about 20 liters per second by the insertion of a restrictive baffle in the pumping line. The impedance in the pumping line makes the pumping speed geometry-limited rather than ion-pump-limited. Thus, in the quadrupole, the partial pressures of the admitted gases are essentially independent of their pressures in the ion pump. Mercury vapor is admitted from an appendage, not shown. The conductance from the mercury droplet to the system is adjusted to give a suitable pressure of mercury in the quadrupole when the droplet is at room temperature. Two additional gas inlet systems are provided. They permit the admittance of two gases at rates which are completely independent. During the experiment a chosen gas is admitted at a slow rate, while hydrogen is admitted at variable, faster rates. This simulates the analysis of the effluent from a gas chromatograph.

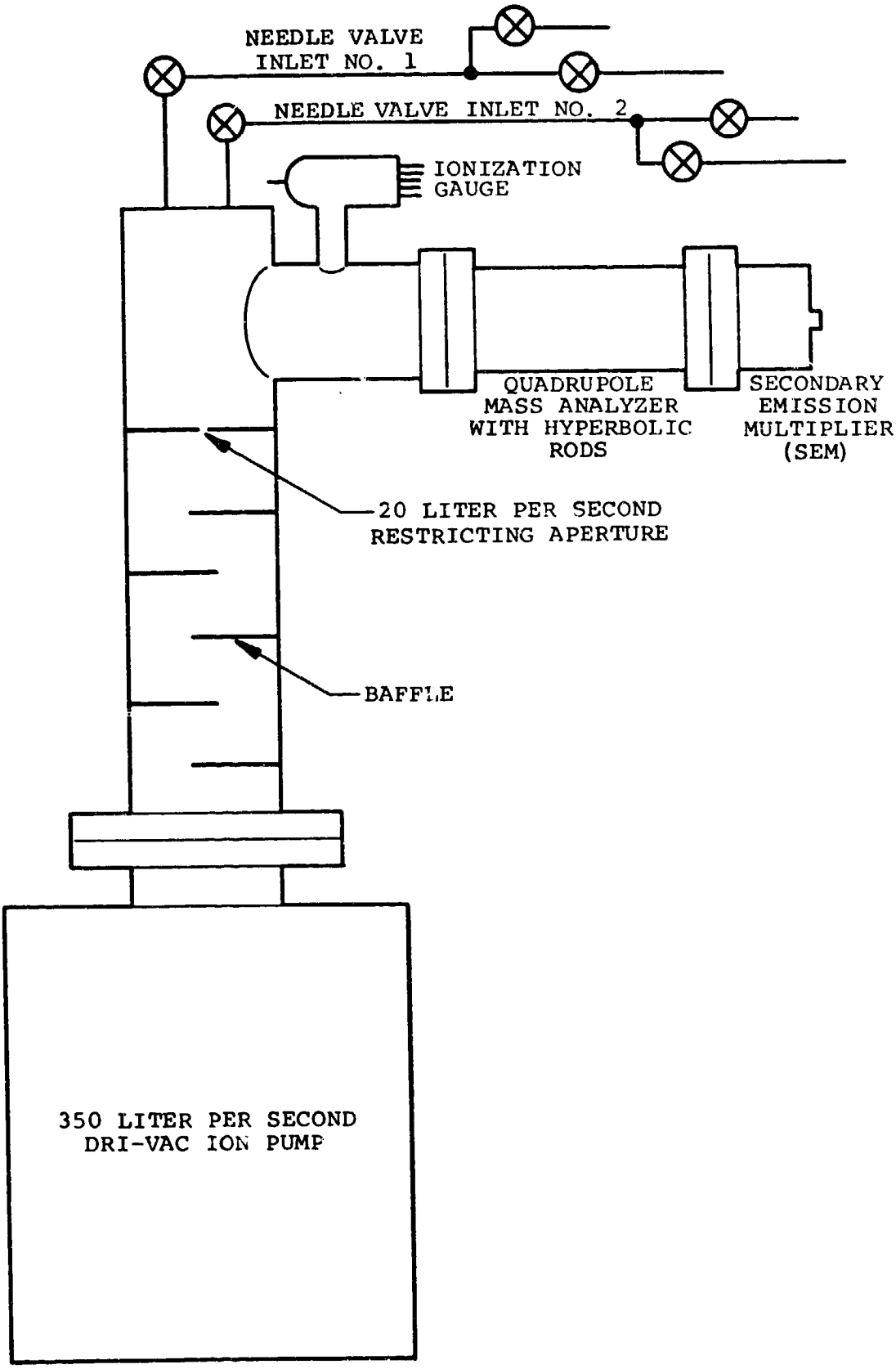


Figure 8. Block Diagram of Vacuum System

## Electronics

The electronic apparatus consists of several sections as shown in Figure 9. Details of these sections are described below.

Crystal Oscillator, Modulator and Power Amplifier. The crystal oscillator and power amplifier operate at 0.500, 0.707, 1.0 and 1.414 MHz. The constant amplitude ac voltage from the crystal oscillator is amplified by varying amounts to achieve the desired excitation levels on the quadrupole. The amount of amplification is controlled by the scanning voltage. The maximum power available from the plate-tuned power amplifier is about 90 watts. This allows continuous scanning to mass 220 at 1.414 MHz. The output is link-coupled through a 52-ohm coaxial transmission line to the quadrupole tank coil.

Quadrupole Excitation Tank Coil. An rf transformer (tank coil) is located in the immediate vicinity of the quadrupole. It provides the necessary impedance match between the transmission line and the resonant circuit of which the rod and segment capacitance is a major part.

High Frequency Rectifiers. A dc feedback voltage for the control unit is provided by two full wave shunt rectifiers which are capacitance coupled to the tank coil. This voltage controls the modulator to keep the ac potential stable and proportional to the scanning control voltage and to stabilize the dc/ac ratio. The negative feedback voltage is compared with its respective control voltage at the input of a high-gain operational amplifier.

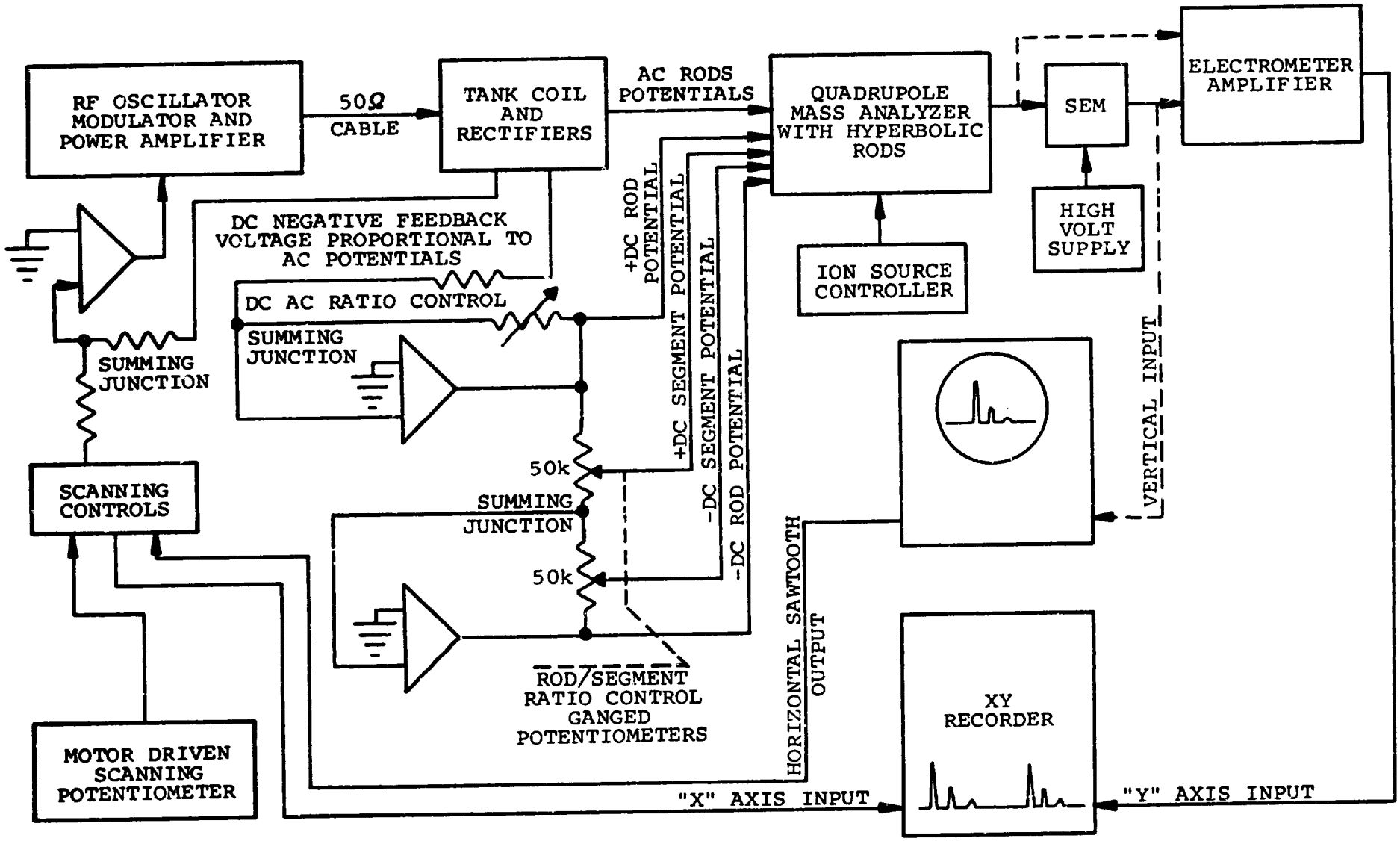


Figure 9. Functional Block Diagram of Electronic Apparatus

Ion Detection. Ion current transmitted through the quadrupole is collected with a Faraday Cup or a secondary emission multiplier. For visual display, the output of the multiplier is connected directly to the vertical input of the oscilloscope. When the XY recorder is used, the output from either the Faraday Cup or multiplier is amplified by means of a capacitance modulated electrometer amplifier. In this case, minor stray currents resulting from electrons are eliminated by placing the Faraday collector about 22 volts negative with respect to ground. The output of the electrometer is connected to the Y-input of an XY recorder. As the X axis of the recorder represents the scanning voltage, a direct plot of ion current as a function of mass number is achieved.

## OPERATION OF THE QUADRUPOLE AT HIGH PRESSURE

### Discussion

When a mass spectrometer is used in conjunction with a gas chromatograph, the composition of the effluent is dominantly that of the carrier gas. It is desired that the dynamic range of the mass spectrometer be as large as possible. That is, it should respond normally to the presence of a component gas at low concentration in the presence of the light carrier gas at high concentration. The largest dynamic range is obtained when the pressure of the chromatograph effluent in the ion source is high.

### Theory

Every mass spectrometer system consists of three portions whose functions are distinctly unique. These are: source, mass analyzer, and detector. It is expedient to discuss the manner in which a high background pressure of a light gas may influence the operation of each of these.

The Source. The presence of a high density of ions of the background gas contributes greatly to the space charge in the ion sourc and alters the potential distribution appreciably. The influence of space charge (owing to electrons and to positive ions) upon the potentials in linear ion sources is considered in a publication by Brubaker[1]. A copy of this paper is included in the Appendix.

---

(1) Brubaker, Wilson M., "Influence of Space Charge on the Potential Distribution in Mass Spectrometer Ion Sources," Journal of Applied Physics, Vol. 26, No. 8, August 1955, pp. 1007-1012.

It is noted that the presence of ionizing electrons depresses the potentials throughout the volume of the source, while the presence of the positive ions raises the potentials. Further, there is a critical pressure at which these two opposing factors just cancel each other in the ionizing plane. At pressures higher than critical, the presence of the positive ions dominates, and the potentials throughout the source become more positive than they are under conditions of zero space charge. In the experiments described in this report, the critical pressure is about $2 \times 10^{-3}$ torr. The source potentials were such that the ion current from the source is highly dependent upon the ion acceleration potential. That is, it is strongly influenced by the potential of the ionization region. Since the ion density increases as the pressure of the background gas is raised, it is anticipated that the ion current from the source is a weak function of the pressure of the hydrogen gas. It is a weak function because the background pressure has only a very weak influence on the potentials in the source.

These considerations lead to the conclusion that the sensitivity of the ion source to all gases increases slightly as the pressure of the gas in the source becomes quite high (above $2 \times 10^{-3}$ torr).

Another influence of space charge is to spread the ion beam as it enters the quadrupole. Since the paths of ions of all masses are identical in static electric fields, a calculation of the trajectory of a hydrogen ion on the periphery of the ion beam describes the trajectories of the heavy ions as well. The hydrogen ions remain in the ion beam until they are driven to the rods by the ac fields.

The Analyzer. Once the ions leave the source and enter the analyzer, the influence of a high background pressure of a gas of low mass on the performance of the device is associated with the collisions made between the ions and the neutral molecules. Energy and momentum are conserved in each collision, but the collisions need not be elastic. In addition to collisions and the changes made in the trajectories of the colliding particles, there is also the possibility of charge exchanges. That is, the ion may become neutralized by contact with a neutral molecule of lower ionization potential. When the carrier gas is helium, there is no possibility of a charge exchange from a "sample" ion to a neutral helium molecule, because the ionization potential of helium, 24.5 volts, is higher than that of any other molecule. The ionization potential of hydrogen is 13.5 volts. Very few species of molecules have higher ionization potentials, so the probability of a charge exchange from the sample ion to the hydrogen molecule is negligible.

The quadrupole mass analyzer is less vulnerable to the effects of gas scattering of the ions in the analyzer than the magnet or "ray" machines. In the latter, small angle scattering can cause ions which should miss the exit slit to pass through it. In this manner, the width of the peak is broadened. This broadening lowers the resolving power and limits the capability of the instrument to respond to a small peak adjacent to a large one. In the quadrupole, small angle scattering has a negligible probability of causing an ion to be transmitted if its working point lies in the unstable portion of the stability diagram. Rather, the small angle scattering (all collisions of mercury or potassium ions with hydrogen molecules result in small angle scattering for the heavier ions) is more likely to influence the operation of the

quadrupole by making a change in the axial component of velocity. The radial velocity of the ions approaches that which is appropriate for ions which have been accelerated by the peak applied ac potential. This is very large relative to the axial component of velocity, which results from the accelerations in the ion source. Thus, even a small angle scattering of a mercury ion by a hydrogen molecule may cause it to be returned to the source end of the quadrupole.

These considerations lead to the conclusion that operation of the quadrupole mass analyzer at high pressure results in a loss of sensitivity with little change in the resolving power.

The Detector. Since the detector is a device which responds to the transmission of ions through the quadrupole, it would seem that it is unaffected by the density of the gas in which it operates. Unfortunately, this is not necessarily the case. If the detector is a secondary emission multiplier, it is essential that the pressure remain sufficiently low that the rate of ion production by the cascading electron stream be negligible.

Another potential influence of high pressure on the operation of the detector is the photon beam which emanates from the ionizing region in the ion source. These photons travel through the quadrupole, releasing electrons at the end of their paths. Photo-ejected electrons which leave a Faraday Cup detector provide electrical signals which are indistinguishable from those produced by the neutralization of incident

positive ions. As the data of these experiments indicate, this is a real phenomenon. When the collector is a Faraday Cup, impressed fields can be used to suppress the photo-ejected electrons, and to return them to the cup. However, when a secondary emission multiplier is used, this cannot be done because the electrons are released at the first dynode by the impingement of energetic ions. These may not be suppressed, as they constitute the signal.

## Hydrogen Pressure-Related Background Current

The Findings. As the pressure of hydrogen is raised to the higher levels, there appears a background current which is independent of many of the variables which influence the ion currents. This current appears at high hydrogen pressures when the excitation of the quadrupole is essentially that required for the display of the mercury spectrum. It is present when the working points associated with the mercury isotopes are external to the stable portion of the stability diagram. That is, the ac potential may be that appropriate for the transmission of one of the mercury isotopes, and the dc potential may be such that the working point lies above the apex of the diagram; otherwise, the working points may lie on the scan line which cuts the diagram below the apex, but which lie outside the stable portion, on either side. This background current appears as a steady signal on top of which the spectral peaks appear.

Experiments made with the background current revealed:

1. It is proportional to the hydrogen pressure.
2. It is proportional to the ionizing electron current.
3. It is independent of the magnitude of the ac potentials applied to the rods over a wide range.
4. It is independent of the density of the ion current from the source.
5. It is independent of the potential of the ion collector in the interval of zero to minus 22 volts.

Interpretation of the Findings. The relations between the background current and the various operating parameters indicate that the current is caused by photons from the ion source. Further, these photons are associated with the ion production rate, but not with the rate of ion emission from the source. The origin of these photons appears to be excited hydrogen molecules or atoms.

Significance of the Background Current. If the background, ion-unrelated current were really a steady one, it could be subtracted from the output, leaving only the true ion current signal. However, there is no such thing as a "dc" current which has a constant, nonfluctuating value. There is always a statistical fluctuation which is due to the randomness of the electron flow.

A first order derivation of the magnitude of the statistical fluctuation in a "dc" current follows. Let $(dn/dt)_o$ be the long-term average number of charges which flows each second.

It is related to the "dc" current i by $i = (dn/dt)_o e$. The average number of charges which arrive at the collector in a time $t_1$ is

$$n = (dn/dt)_o t_1$$

The statistical fluctuation in this number, $\delta n$, is given by

$$\delta n = \{(dn/dt)_o t_1\}^{0.5}$$

The fractional deviation is

$$\delta n/n = \{(dn/dt)_o t_1\}^{-0.5}$$

Since the current is proportional to the number of charges which arrive in time $t_1$,

$$\delta i/i = \delta n/n = \{(dn/dt)_o t_1\}^{-0.5}$$

and

$$\delta i = 4 \times 10^{-10} (i/t_1)^{0.5}$$

In these tests, the background current was about $9 \times 10^{-14}$ amperes when the hydrogen pressure was $4 \times 10^{-5}$ torr. As a worst case, assume that the pressure in the source is $5 \times 10^{-4}$ torr. This would have an associated background current of $1.1 \times 10^{-12}$ amperes. In this case, the uncertainty in the current observed during a time $t_1$ becomes

$$\delta i = 4.2 \times 10^{-16} (t_1)^{-0.5}$$

The calculated variation in ion current can be related to an uncertainty in the pressure by the observance that an anticipated sensitivity of the quadrupole system is in the order of $10^{-5}$ amperes per torr. Thus,

$$\delta p = 4.2 \times 10^{-11} \ (t_1)^{-0.5}$$

This represents a limiting dynamic range of about $10^7$ when the pressure in the ion source is above $10^{-4}$ torr, and the time for scanning one peak is about 1 second.

The uncertainty in the ion current calculated above represents the contribution of the background current fluctuations to the "noise" in the output signal. There are many additional factors which influence the low partial pressure limit of an observed molecular species. These include all of the noise generators in the detection system. If a secondary emission multiplier is used, it makes a very significant contribution. Further, the other amplifiers in the read-out system make their individual contributions.

Mass Spectra at High Hydrogen Pressure

Observationally, as one raises the pressure of a background gas while observing the spectrum of a different gas at a lower, constant pressure, he sees certain changes in the appearance of the spectrum of the reference gas. It is of interest to know which of the three components of the spectrometer is responsible for these changes. However, it is most difficult to arrange experiments which yield results that identify the locus of the cause of the observed spectral changes. One reason for this is the relative immunity of the quadrupole mass spectrometer to degrading influences of high background pressure.

One of the critical problems associated with this experiment is that of maintaining constant the pressure of the reference gas. The system used in these experiments is evacuated by an ion pump. Since the operating pressure of these devices is limited to pressures below about $5 \times 10^{-5}$, a severe constriction is placed in the pump line. This permits the hydrogen pressure in the quadrupole to be about fifty times higher than it is in the pump. It was anticipated that this large amount of differential pumping would assure a constancy of the pressure of the reference gas. Unfortunately, this is not the case. When titanium is pumping hydrogen at a very high rate, the resulting mechanical forces seem to open fissures from which previously pumped gases emerge. This phenomenon limits the accuracy of the experimental results obtained. The quadrupole itself operates so well at high pressure that a relatively small variation in the pressure of the reference gas becomes an important factor.

Experiments with Mercury Spectrum. Mercury vapor is well-suited to provide the reference spectrum because there are no background gases of similar mass to produce interfering spectra. It is introduced into the system through a small capillary of appropriate dimensions to provide a partial pressure of the mass 202 isotope of about $1 \times 10^{-7}$ torr when the mercury temperature is 20°C. A thermometer attached to the mercury supply and insulated from the external environment provided data from which all mercury ion currents are normalized to 20°C. The ion source parameters that were previously used in the comparison between round and hyperbolic rod quadrupoles were again used in these experiments. This provides an indicated sensitivity of about $3.5 \times 10^{-5}$ amperes/torr for 2 volt ions. Under

these conditions, good resolution of adjacent peaks at mass 200 is achieved at adequate sensitivity.

The procedure used in collecting the data is as follows: (1) The peaks at mass 201 and 202 are recorded at background pressure. (2) Hydrogen gas is then admitted to a significantly higher pressure. The partial pressure of hydrogen is determined from the difference between the ionization gauge readings before and after admitting hydrogen. (3) The pump pressure as indicated by pump current is allowed to stabilize to a point where the ratio of quadrupole to pump hydrogen pressures approaches 50 to 1. (4) Mass peaks 201 and 202 are recorded at this new pressure and steps 2, 3, and 4 are repeated until the pump can no longer stabilize. At this time the hydrogen pressure in the quadrupole is about $4 \times 10^{-4}$ torr.

Measurements of peak heights and widths are made directly from the XY plots with the aid of a decimal scale. Normalizations are made of the peak heights at 100 percent transmission to compensate for small drifts in the pressure of the mercury vapor.

Using mercury as the reference gas, data have been obtained which relate peak heights to resolving power at various hydrogen background pressures. These data are presented in Figure 10. While these data do not identify the location of the pressure dependence in the mass spectrometer, they do show the manner in which high hydrogen pressures influence the operation of the entire instrument. Degradation of the performance is quite apparent at $10^{-4}$ torr, and increases rapidly as the pressure is raised above this level.

Experiments with Potassium Spectrum. The electron bombardment ion source was replaced by a thermal source. Potassium chloride was placed on a tungsten ribbon to form this source.

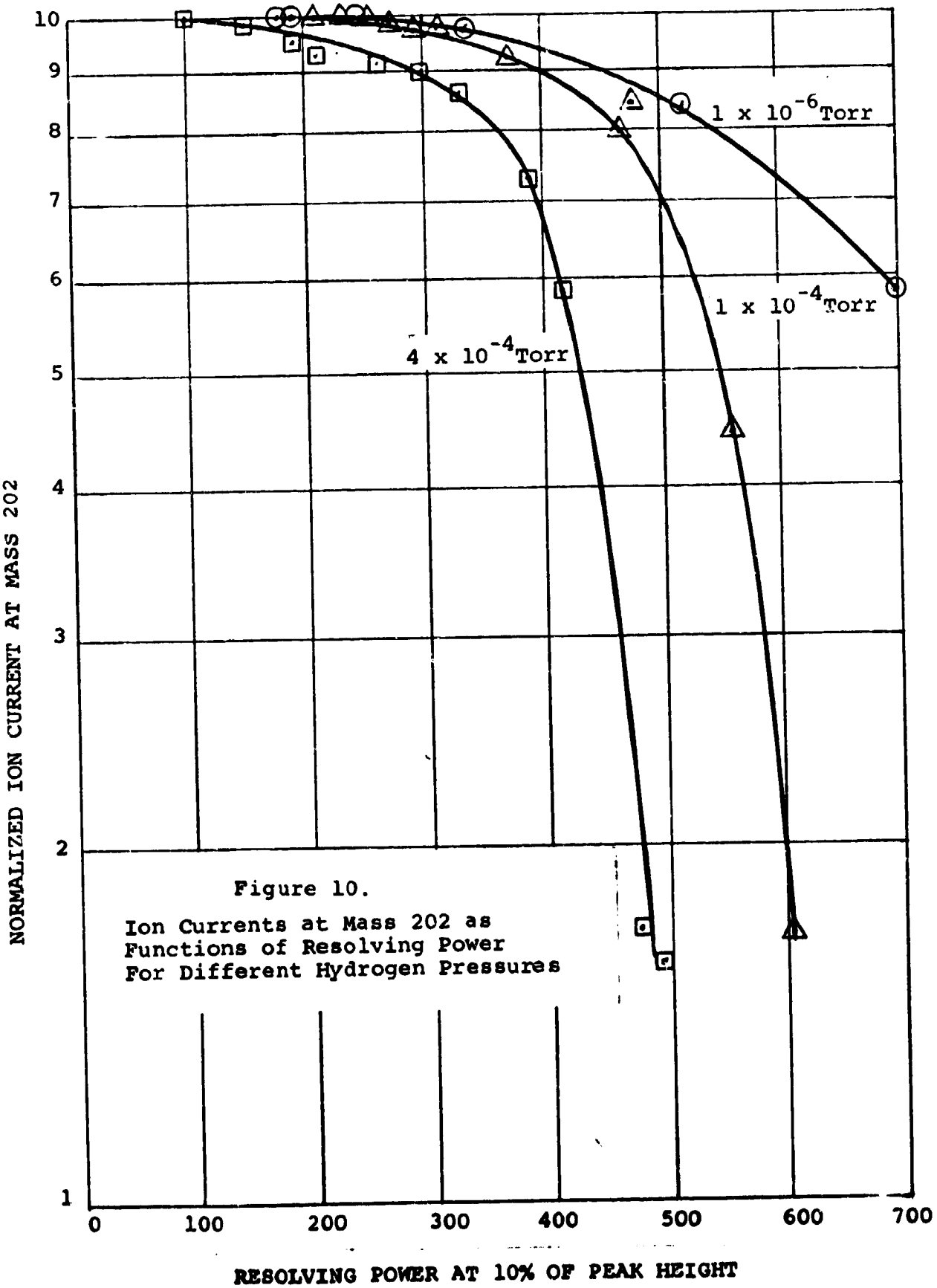


Figure 10.

Ion Currents at Mass 202 as Functions of Resolving Power For Different Hydrogen Pressures

Under these conditions, there was little relation between the intensity of the incident reference spectrum upon the quadrupole entrance aperture and the pressure of hydrogen. With this apparatus, the pressure of hydrogen can be raised to very high values without disturbing the ion source.

The geometry of the thermal ion source is shown in Figure 11. A grid is placed between the filament and the entrance aperture for the purpose of monitoring the ion current from the source. Since the ionic emission varies so rapidly with temperature, the observation of the emission at high pressures was desired. Simple calculations of the power required to raise the incident hydrogen molecules to the ribbon temperature reveal that at a pressure of $10^{-3}$ torr it is less than 10 milliwatts. This is so small relative to the several watts which are applied to the same area under operating conditions that it is entirely negligible. Experimentally, there was no correlation between the ion current drawn to the grid and the hydrogen pressure.

The results of this experiment are shown in Figures 12 and 13. Here the resolved ion current at the collector and the resolving power of the instrument are plotted as functions of the hydrogen pressure for the resolving powers of 40 and 100. As anticipated in the theoretical considerations, the resolving power of the instrument is unaffected by a high density of neutral molecules in the quadrupole mass analyzer. The ionic transmission suffers as the pressure is raised to the high values. However, the attenuation is modest for an operating pressure of $10^{-3}$ torr.

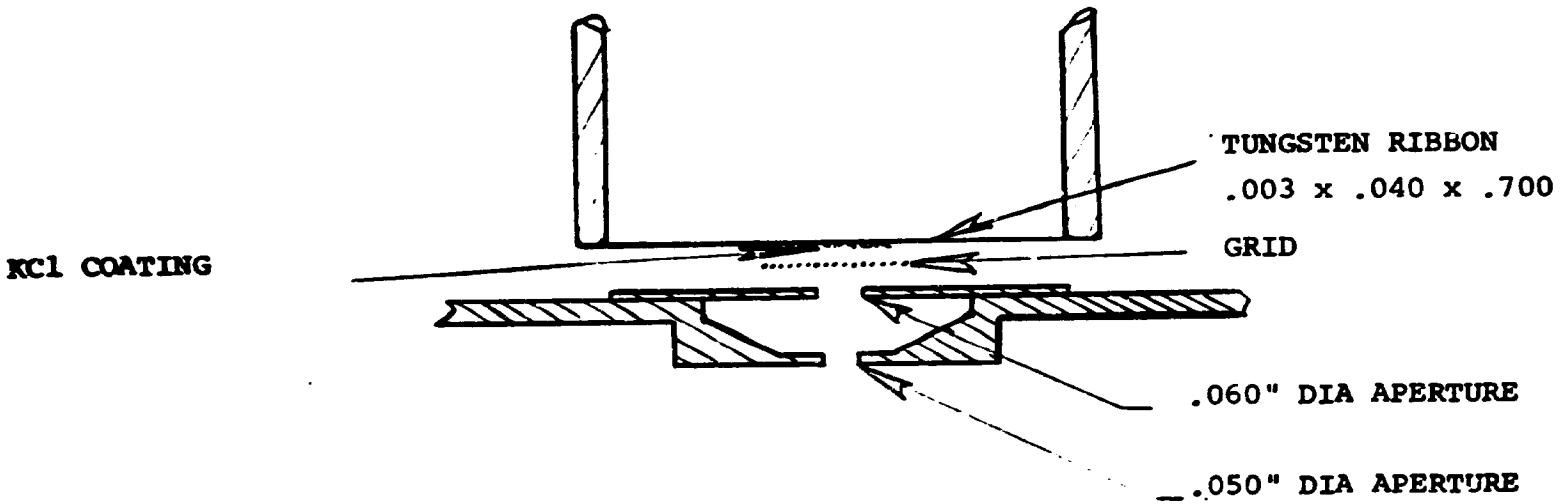


Figure 11. Thermal Ion Source

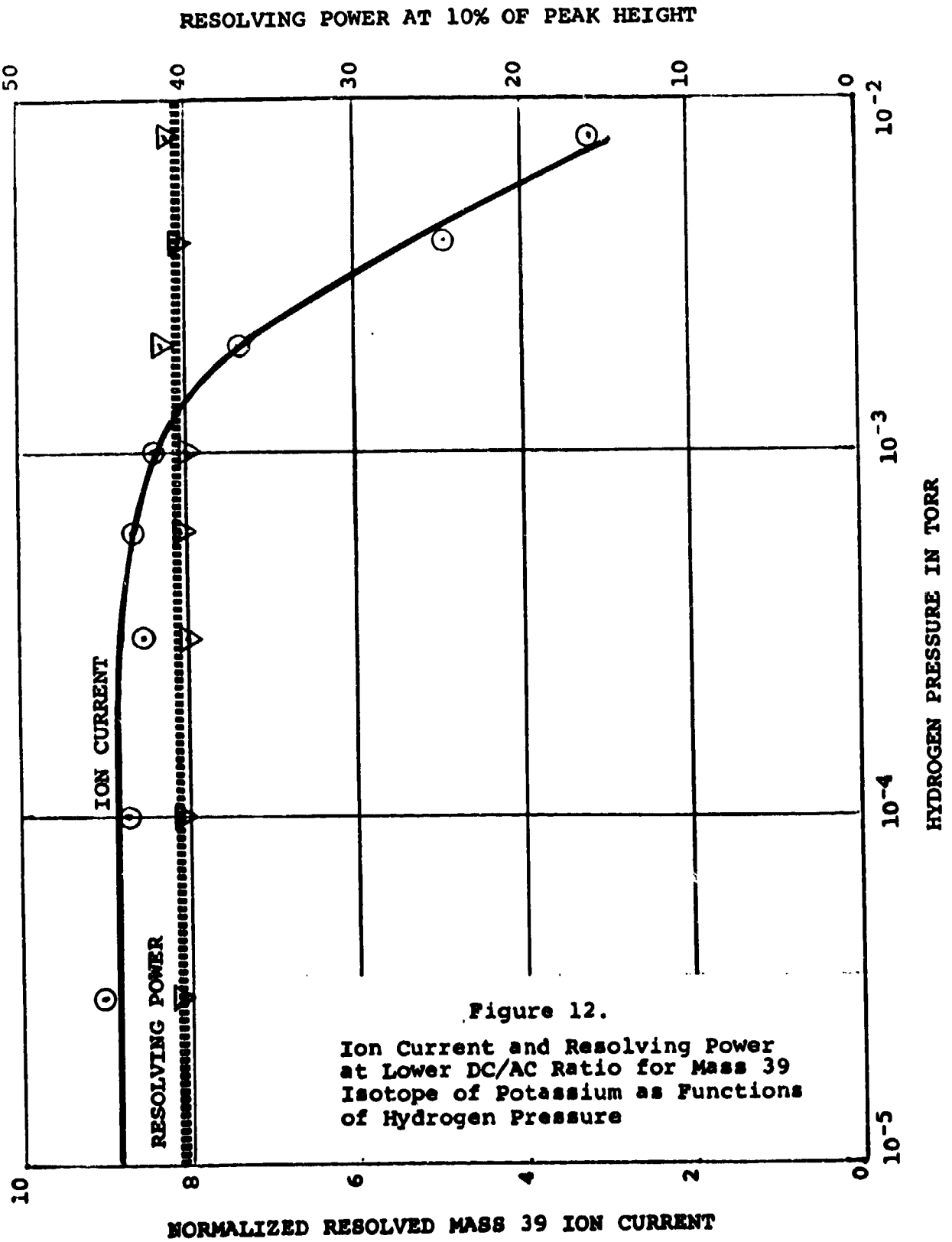


Figure 12.

Ion Current and Resolving Power at Lower DC/AC Ratio for Mass 39 Isotope of Potassium as Functions of Hydrogen Pressure

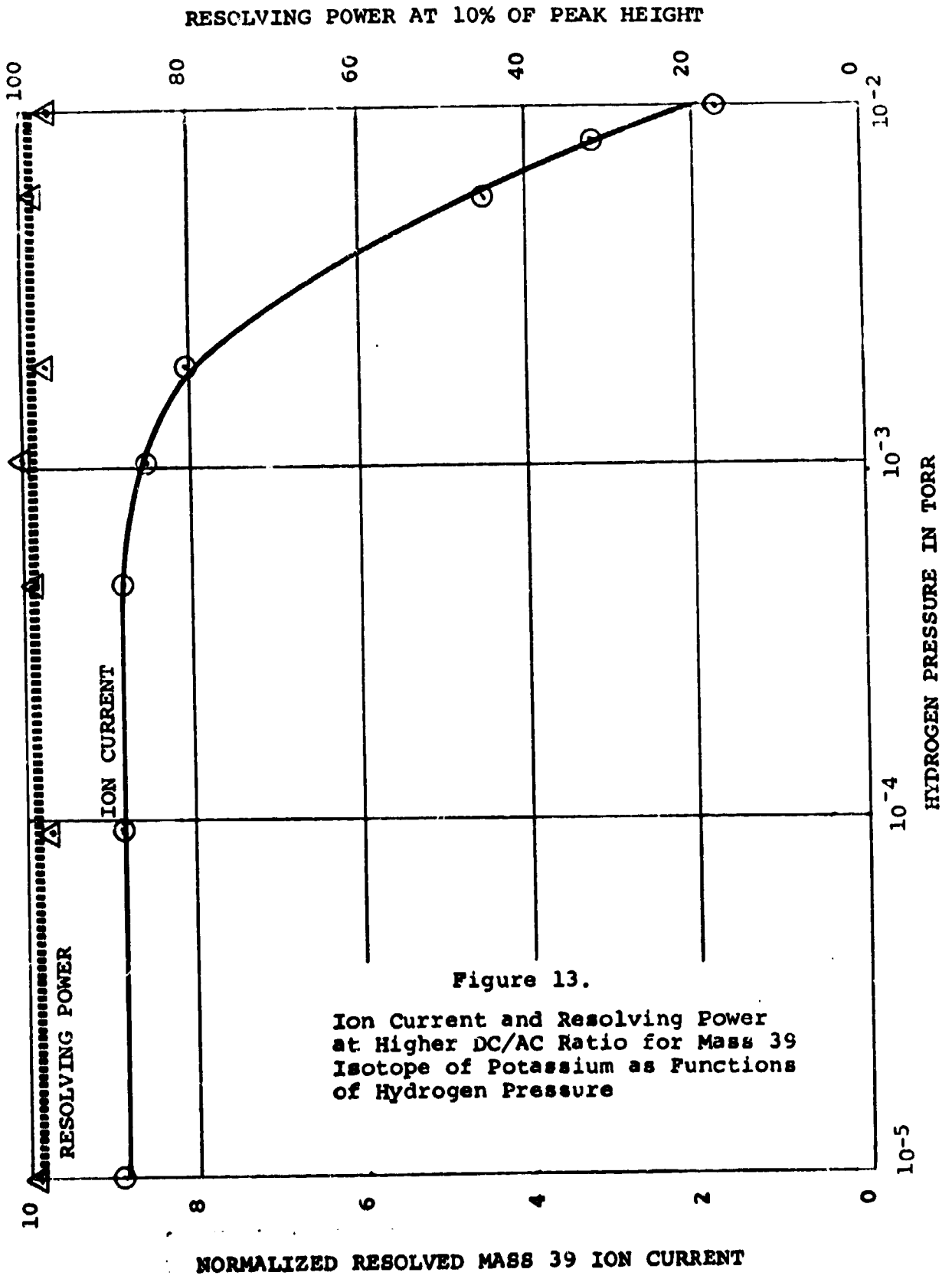


Figure 13.

Ion Current and Resolving Power at Higher DC/AC Ratio for Mass 39 Isotope of Potassium as Functions of Hydrogen Pressure

## MASS DISCRIMINATION IN QUADRUPOLE MASS SPECTROMETERS

### Discussion

Since the term "mass discrimination" does not appear in the index of any of four of the recently written books on mass spectrometers, a definition is in order.

For the purposes of this investigation, "mass discrimination" is considered to be the mass dependence of the probability of an ion, once formed, to be registered as a transmitted ion at the output of the detector. This excludes ionization cross section and cracking patterns as mass discrimination factors.

The quadrupole, as any other mass spectrometer, consists of three distinct sections, each with its own specific function. These are the source, the mass analyzer, and the detector. The possibility of mass discrimination in each of these sections is explored. Additionally, it is found that mass discrimination may occur in the fringe fields between the source and the mass analyzer.

### Theory

The Ion Source. The potentials applied to the ion accelerating electrodes of the source are not given any ac components. The fields to which the ions respond result from dc potentials applied to electrodes, to space charge of electrons and ions, and to surface charges which may reside on insulating layers on the electrodes. Since the design of ion sources is not conducive to the generation of ac potentials, it may be assumed that the fields in quadrupole ion sources are static in nature. (Static means the absence of periodic variations with time.)

It is readily shown that the trajectory of a charged particle which starts from rest in a static electric field is independent of the mass of the particle. If an ion is moving in a curved path and $E_\rho$ is the component of the electric field along the radius of curvature, its magnitude is related to the radius of curvature, $\rho$, by

$$e\ E_\rho = \frac{mv^2}{\rho} = \frac{2\ Ve}{\rho}$$

V is the potential through which the particle is accelerated from rest to a velocity v. From these two equations

$$\rho = 2\ \frac{V}{E_\rho}$$

Since the above consideration applies to any path segment, it holds for the entire path. The radius of curvature is independent of the mass of the ion.

The trajectories of ions which start from rest under the influence of static electric fields traverse paths which are identical for all masses. Thus, the emergent ions from the non-magnetic dc sources used on quadrupole mass spectrometers follow paths which are the same for all masses.

At the moment of its ionization, a molecule is moving with thermal energy. Temperatures of ion source electrodes are the order of 500°K. Since one electron volt is equivalent to nearly 12,000°K, a temperature of 500°K corresponds to about 40 millivolts. This potential is negligible relative to the energies given ions very early in their paths.

For most molecular species the removal of an electron by electron bombardment results in the formation of an ion

with a velocity equivalent to the velocity the molecule had before ionization. This occurs for the parent ion of a simple gas ($O_2^+$). More complicated molecules, like those of some hydrocarbons, are formed with more than a volt of kinetic energy. When this happens, the probability of the ion reaching the collector is lessened for any mass spectrometer. This type of mass discrimination is recognized, but is not explored in the work described by this report.

The production rate of ions of any given species is proportional to the volume density of the parent molecule and to the ionization cross-section. Because ionization cross-sections are specific to the molecule and the energy of the bombarding electrons, the intensities of the ion peaks are not the same for all species. However, this phenomenon is not mass discrimination according to our definition.

Fringe Fields. It has been shown(2) that as an ion traverses the fringe fields between the source and the strong fields within the conventional quadrupole, it receives a y-directed impulse which is a function of the number of cycles (periods) which occur during the traversal. Computer studies(2) of ionic trajectories have shown the relation between the normalized amplitude and the number of cycles spent in the fringe field to be

$$A_{max} = 0.34 \text{ (Resolving Power)}^{\frac{1}{2}} \times 10^{0.25n}$$

where n is the number of periods it takes the ion to cross the fringe field. The equation is valid for $n \geq 2$.

(2) Final Report NASW-1298, p. 17.

Studies of ionic trajectories in quadrupole mass filters[3] have shown that the paths are the same for all masses if all potentials hold a constant relationship to the mass of the transmitted ion. The definitions of a and q:

$$a = \frac{8e\ V_{dc}}{m\ r_o^2 \omega^2} = \frac{8e}{r_o^2 \omega^2}\ \left(\frac{V_{dc}}{m}\right)$$

$$q = \frac{4e\ V_{ac}}{m\ r_o^2 \omega^2} = \frac{4e}{r_o^2 \omega^2}\ \left(\frac{V_{ac}}{m}\right)$$

and the expression for the axial velocity $v_z$

$$v_z = \sqrt{\frac{2V_{acc}e}{m}} = \sqrt{2e}\ \sqrt{\frac{V_{acc}}{m}}$$

reveal that the transit time and the loci of the working points of the transmitted ions all are unchanged during a mass scan if all accelerating voltages remain proportional to the mass of the transmitted ions.

When the trajectories are mass invariant, the spectrum appears as from a magnetic analyzer: m/dm is constant. If the ion accelerating potentials in the source are held constant, the resolving power, m/dm, is nearly proportional to m. That is, dm $\approx$ constant. This is a preferred manner of operating the quadrupole mass filter. This introduces an important non-scanning dc potential. Since the trajectories are now mass dependent, the transmission efficiency becomes a function of mass. That is, an amount of mass discrimination exists.

(3) Final Reports NASW-1298 and AF 19(604)-5911.

A non-scanning, constant ion energy causes the time spent by the ion in traversing the fringe fields to be proportional to the square root of the mass-to-charge ratio of the ion. The greater number of ac periods which occur during the transit of the heavier ions causes an increased deflection of the trajectories in the y-direction. This circumstance severely attenuates the transmission probability for heavy ions in the conventional quadrupole, because more than two ac cycles occur during their transit of the fringe fields.

The fringe field is not a source of mass discrimination in the delayed dc ramp mode[4] because the working point moves through the stable portion of the a-q diagram as the ion enters the quadrupole.

Quadrupole Mass Analyzer. There should be no mass discrimination in a normally operating mass filter for ions which enter along identical trajectories. However, the presence of non-scaling dc potentials affects the trajectories in manners which are mass dependent. Non-scaling dc potentials may be of two kinds. They may be added to the mass-proportional dc potentials which are normally applied. They also may be due to surface potentials on the rods. These result from ion (or electron) bombardment of insulating layers on the field-forming surfaces.

On the conventional quadrupole, a non-scanning dc potential can be used to offset the mass discrimination caused by the fringe field. Because of the vastly different manners in which these two factors influence mass discrimination, it is highly unlikely that an effective cancellation over an appreciable mass range is obtainable.

(4) Final Report NAWS-1298.

Mass discrimination caused by surface charges is difficult to evaluate quantitatively because of the possible variation in the sign and location of the charge. Ions heavier than the transmitted ones are deposited on the y-rods, and vice versa. Thus, the surface charges become functions of the conductivity of the insulating layers and of the time and magnitude of the ionic (electron) bombardment. If the period for a mass scan is short relative to the time constant (RC) of the insulating layer, the resulting perturbations in the field are essentially the same for ions of all masses. In this instance, it is readily seen that the field perturbations are more disturbing to the trajectories of the low mass ions than for the heavy, because the applied potentials are proportional to the ionic mass.

Detector. Computer studies show that ions leave the fields of the quadrupole with large, varying amounts of radial velocities. First order, these velocities are the same for ions of all masses. Since, as the quadrupole is usually operated, the axial velocity is mass dependent, the trajectories as the ions leave the quadrupole are mass dependent. When ions are caught in a Faraday Cup of appropriate geometry, these differences lead to no mass discrimination.

When the detector is a secondary emission multiplier, mass discrimination is present. First, the number of electrons released by an impinging ion is velocity dependent. Ions are accelerated by several kilovolts between the quadrupole and the multiplier. The heavier ions acquire less velocity and release fewer electrons than the lighter ions. This effect is well known.

As the radial component of ionic velocity is nearly the same for all ions, while the axial component varies inversely

as the square root of the mass, light ions strike the multiplier near the axis, the heavier ones more remotely.

When multipliers have been used under conditions that cause a deterioration of the gain in regions of heavy ion bombardment, an additional unpredictable variation in gain which is mass dependent is experience. This type of mass discrimination is difficult to evaluate because there is no readily available manner to measure the multiplier gain as a function of the position of ion impact.

## EXPERIMENTS

In the design of the electronic portion of a quadrupole mass filter, it is necessary to know the manner in which the dc/ac potential ratio must be tailored if mass discrimination is to be avoided when the instrument is operated at less than 100 percent transmission efficiency. Unless this is known and the exciter design matches this requirement, the relative heights of separated peaks will change as a function of the setting of the dc/ac potential ratio adjustment.

Any attempt to provide a theoretical prediction of the mass dependence of the dc/ac ratio must include a great number of factors whose influences are not orthogonal. These factors include the dimensions of the instrument, the frequency of excitation, the energy of the ion beam, and the divergence of the ion beam in both the x and the y directions. Additionally, the diameter of the entering ion beam, in relation to the instrument radius, $r_o$, is also an important factor.

The desired data relate the ratio of the dc/ac potentials for constant transmission efficiencies over an extended mass range. In order to be useful, these data must be obtained at greater accuracy than is obtainable with <u>any</u> ac voltmeter operating in the megahertz frequency range. However, the

quadrupole itself is a most effective voltmeter when the geometrical constants are known. The variation of the dc/ac ratio can be observed without knowing the absolute values. Providing that the value of q at the apex of the peak is the same for all masses, the ac potential at the top of the peak is proportional to the mass of the transmitted ions. Theory predicts that the top of the peak occurs when the working point is on the line $\beta_x + \beta_y = 1$. Since the slope of this line is not infinite (vertical), there is a small shift in q as the dc/ac ratio changes. The associated changes in m, $\Delta m$, have been noted and if the relation

$$V_{ac} = k(m + \Delta m)$$

is used to relate the excitation voltage to the mass of the transmitted ions, then

$$V_{dc}/V_{ac} = V_{dc}/(m + \Delta m)k$$

Hence, by observing the dependence of $V_{dc}/(m + \Delta m)$ on m, the variation in the dc to ac potentials for constant transmission efficiency is found.

Unexpected financial constraints prevented an in-depth study of mass discrimination. Only preliminary experiments were performed.

The quadrupole was operated in a manner slightly different from normal. All data were taken with less than 100 percent transmission with pointed peaks. The output of the instrument was displayed on an oscilloscope. The ac potential was scanned over one mass unit and the corresponding saw-tooth

potential was impressed on the x-input of the scope. The y-input was connected to the output of the secondary emission multiplier. The dc rod potential was adjusted to the constant value which gave the desired transmission efficiency, and was read on a digital voltmeter.

The shift in the position of the mass peak on the scope screen was readily observed and related to the transmission efficiency. To first order the observed shift, $\Delta m$ is proportional to m, as predicted by theory. There appeared, however, a small dependence of the fractional reduced shift, $\Delta m/m$ on the mass of the transmitted ions. This dependence is illustrated in Figure 14. The meaning of the differences is unclear and may be associated with some obscure experimental condition.

The observed data which relate the ratio of dc to ac potentials and mass of transmitted ions, observed as described, are presented in Figure 15. These data do not prove, but are consistent with the hypothesis that if the ratio of dc to ac potentials remains constant over a wide range of absolute values (corresponding to mass of transmitted ions) then the transmission efficiency is independent of mass. Although there is a consistent departure of the data of Figure 15 from horizontal lines, the departure is so small as to be accounted for by any one of a number of unknowns. These include contact potential differences and the uncertain factors which cause the relationship of $\Delta m$ to transmission efficiency to be mass dependent, as shown in Figure 14.

To the extent that these data are representative of quadrupole operation in general, they establish the criterion for specifying the electrical characteristics of the exciter which provides the dc and the ac potentials for the quadrupole. Note the importance of very small changes in the ratio of dc

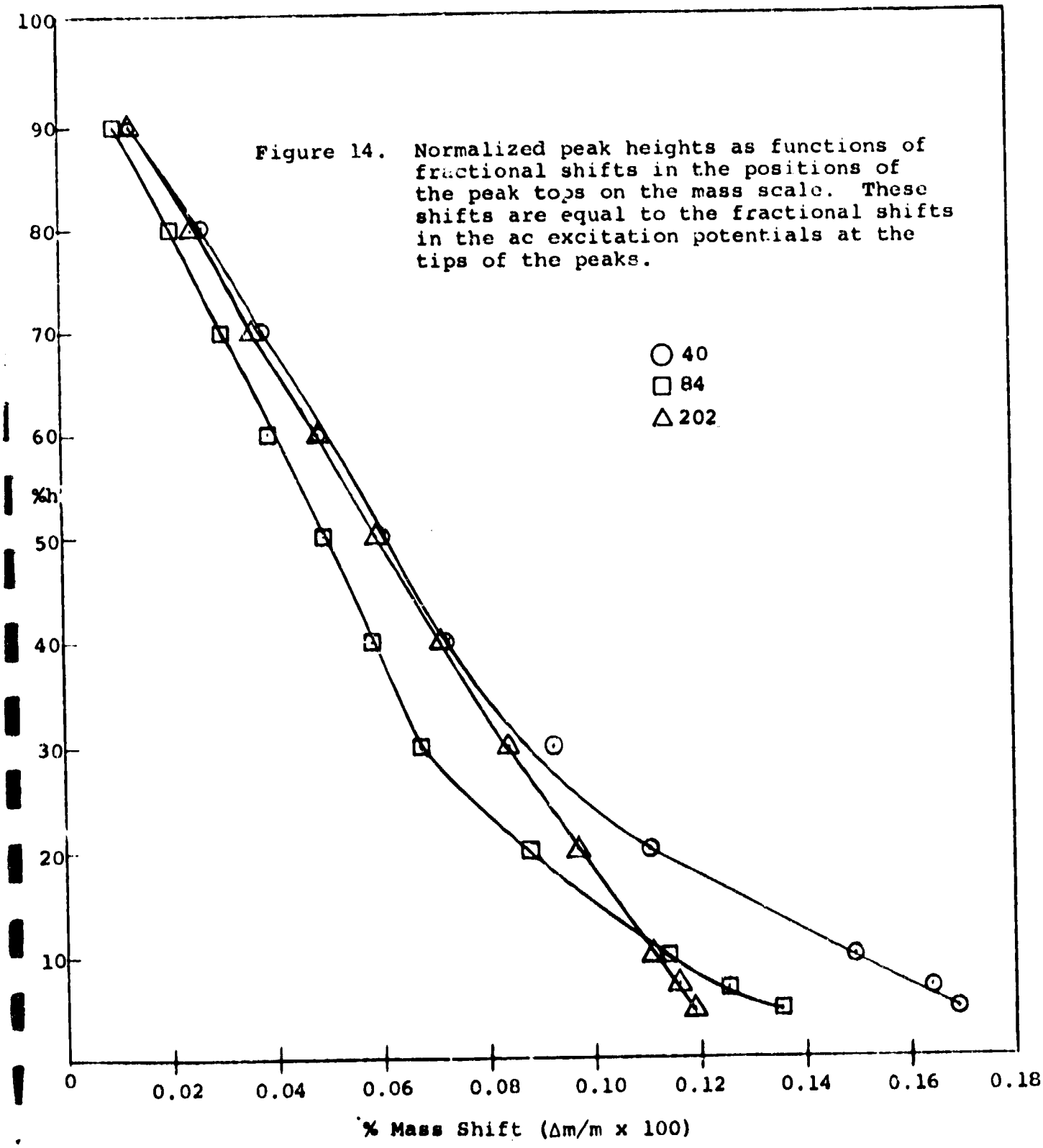


Figure 14. Normalized peak heights as functions of fractional shifts in the positions of the peak tops on the mass scale. These shifts are equal to the fractional shifts in the ac excitation potentials at the tips of the peaks.

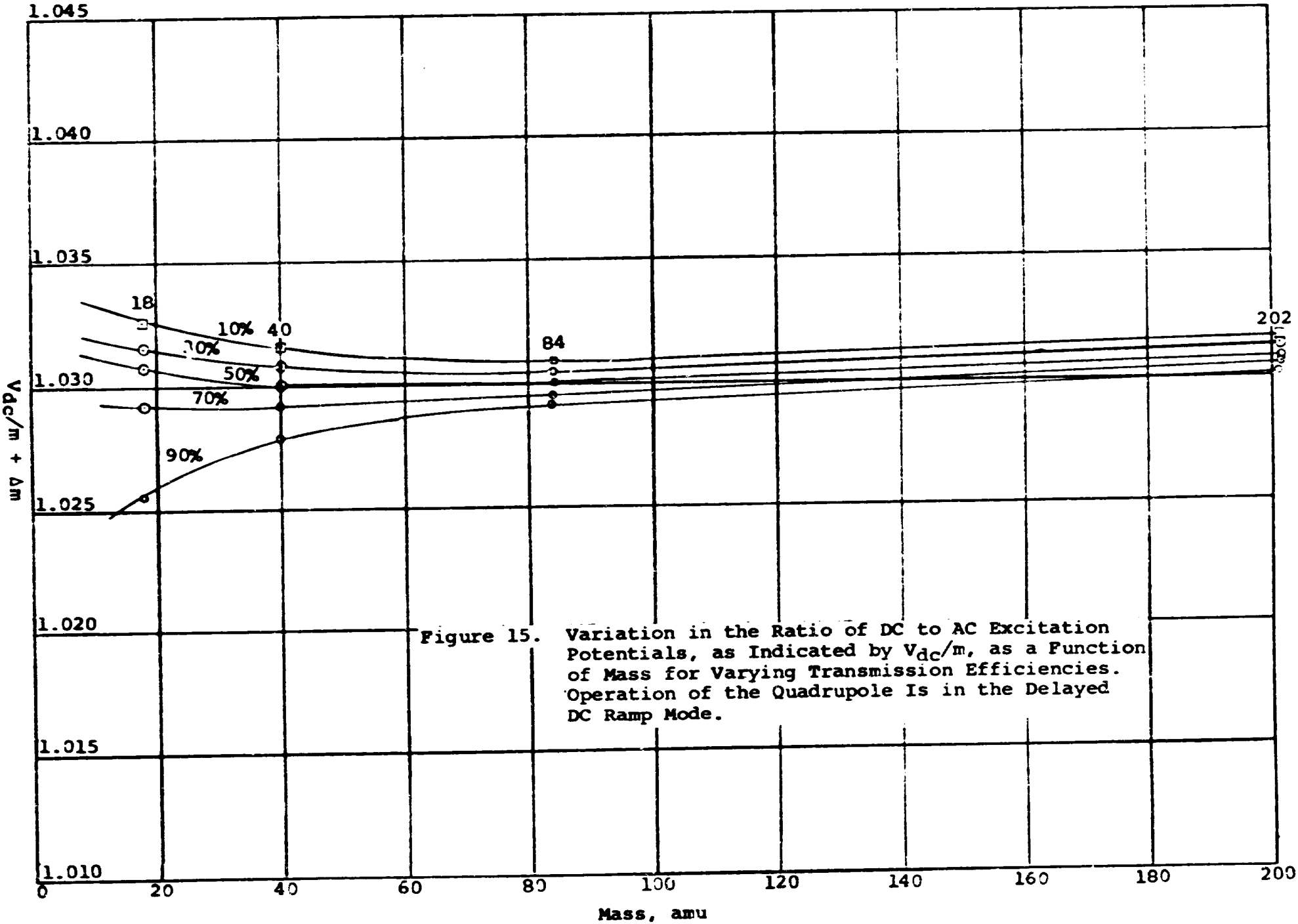


Figure 15. Variation in the Ratio of DC to AC Excitation Potentials, as Indicated by $V_{dc}/m$, as a Function of Mass for Varying Transmission Efficiencies. Operation of the Quadrupole Is in the Delayed DC Ramp Mode.

to ac potentials. Departures of one part in $10^4$ make a significant change in the transmission efficiencies.

It must be emphasized that these data apply to a quadrupole operated in the delayed dc ramp mode where mass discrimination is essentially nonexistent. For operation in the conventional mode, things become more complicated because of the impulses the ions receive as they traverse the fringe fields. These impulses are mass dependent, as discussed earlier.

When a quadrupole is operated in the conventional manner, the mass discrimination against transmission of the ions of high mass can be compensated for (with a sacrifice in resolving power) by decreasing the dc/ac ratio at high mass. However, the amount of the decrease is a function of the ion energy (axial) because the impulse is highly dependent on the transit time of the ions through the fringe field.

An illustration of the discrimination against ions of high mass in the conventional quadrupole is presented in Figures 16 and 17. These two mass scans, from mass 1 to 210, were made in succession. The only known experimental difference in the operating conditions was in the dc potential of the rod segments. The spectrum of Figure 16 was made in the delayed dc ramp mode (zero dc potential on segments), and that of Figure 17 was made in the conventional mode with full dc rod potentials on the segments. The discrimination against ions of higher masses is apparent by the smaller sizes of these peaks in the conventional mode, relative to their heights in the delayed dc ramp mode.

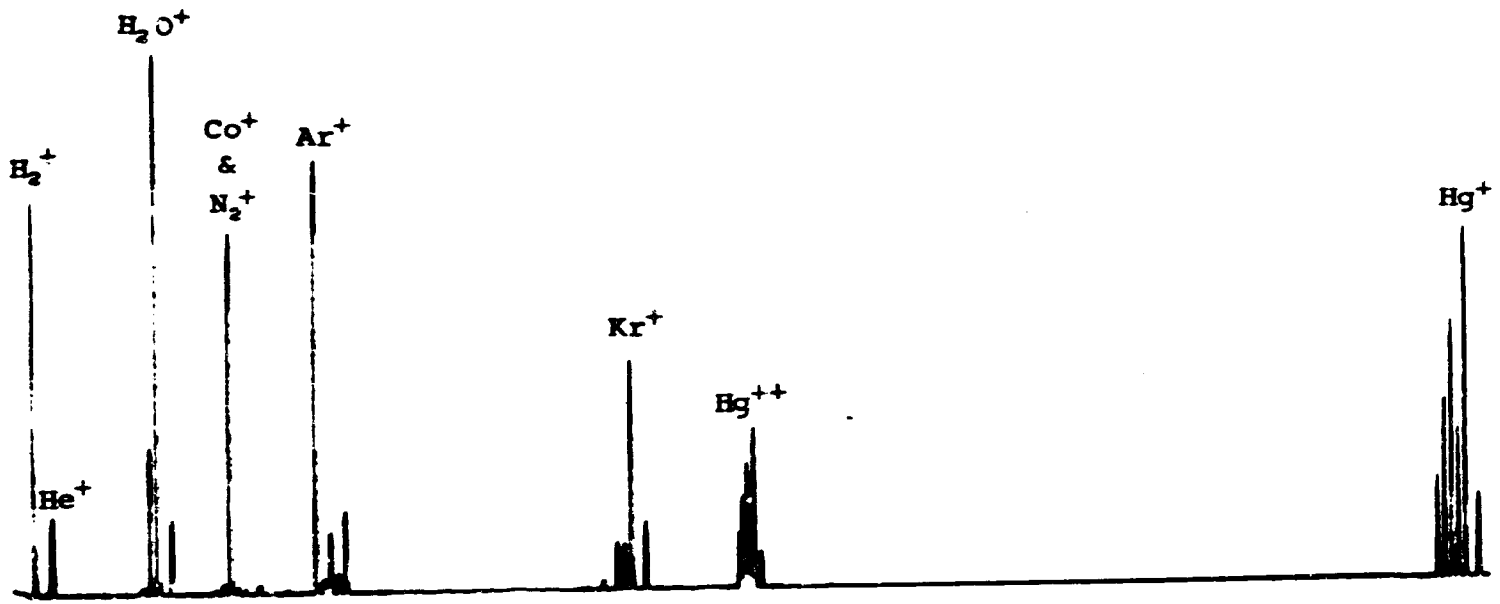


Figure 16. Scan of Wide Mass Range, Delayed DC Ramp Mode

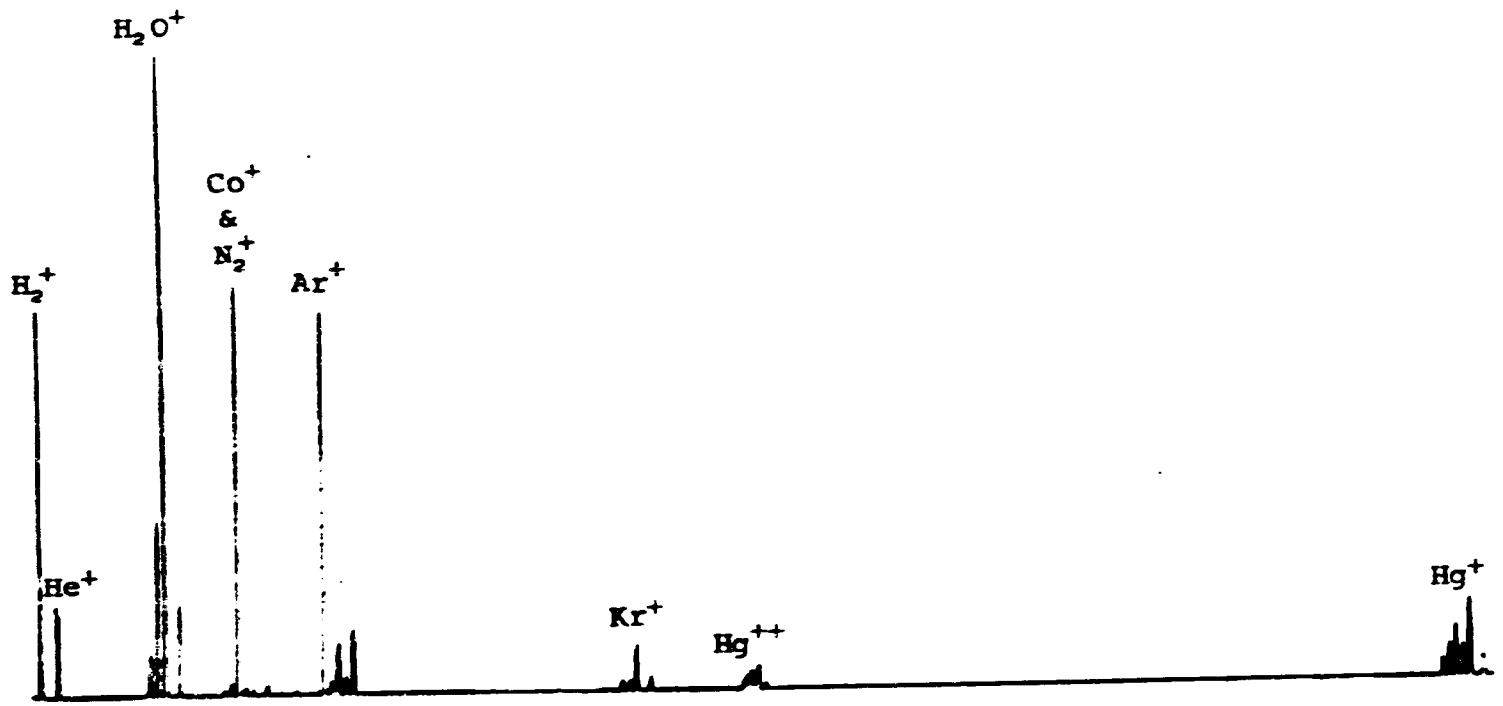


Figure 17. Scan of Wide Mass Range, Conventional Mode

## SUMMARY

Computations of the trajectories of ions through the transition region between two quadrupole assemblies operating at different resolving powers indicate that the trajectories are undisturbed. This fact encourages the use of a tandem quadrupole mass filter.

The addition of hydrogen to a pressure of $10^{-2}$ torr while the quadrupole is displaying the spectrum of a heavier gas has no observable influence on the resolving power when ions are emitted from a thermal source at a rate which is independent of the hydrogen pressure. Transmission efficiency suffers at pressures above $10^{-3}$ torr. When an electron bombardment ion source is used, space charge of the hydrogen ions causes deterioration of the performance to be apparent at pressures above $10^{-5}$ torr.

There appears at the collector a background current which is proportional to the production rate of hydrogen ions, and independent of the transmission of ions through the quadrupole. Its magnitude is about $10^{-9}$ amperes/torr of hydrogen pressure. The average value of this current can be ignored, but the ac component limits the dynamic range of the instrument to about $10^{7}$ when one second is used to observe each mass ion peak. For other mass scan rates, the dynamic range varies as the square root of the time spent on each peak.

Experiments on mass discrimination were interrupted unexpectedly. The preliminary data show that, for operation in the delayed dc ramp mode, there is negligible discrimination in the mass filter if the dc and ac potentials scan in proportion. As predicted by theory and illustrated by practice, there is serious discrimination against ions of heavier mass in the conventional instrument, even when the dc and ac potentials scan in proportion.

## ACKNOWLEDGMENTS

It is a pleasure to acknowledge the support and encouragement given to us on this project by Don Easter and Charles Giffin of NASA Headquarters and JPL. The design and the refinements made in the electronic circuitry by Walter Chamberlin are greatly appreciated. Mr. Chamberlin, assisted by Phil Klasky, operated the apparatus to obtain the experimental data. Fred Pickett provided the necessary maintenance of the apparatus and made minor refinements, such as the thermal ion source.

## REFERENCES


(1) Brubaker, Wilson M., "Influence of Space Charge on the Potential Distribution in Mass Spectrometer Ion Sources," Journal of Applied Physics, Vol. 26, No. 8, August 1955, pp. 1007-1012.

(2) Brubaker, Wilson M., "A Study of the Introduction of Ions into the Region of Strong Fields within a Quadrupole Mass Spectrometer," Final Report for Contract NASW-1298, August 17, 1965 through October 17, 1967.

(3) Brubaker, Wilson M., "Study and Development of the Paul-Type Mass Spectrometer," Final Report for Contract AF 19(604)-5911, April, 1963.

Final Report NASW-1298, See Ref. (2).

(4) Final Report NASW-1298, See Ref. (2).

# APPENDIX I

## Influence of Space Charge on the Potential Distribution in Mass Spectrometer Ion Sources

Reprinted from JOURNAL OF APPLIED PHYSICS, Vol. 26, No. 8, 1007-1012, August, 1955


# Influence of Space Charge on the Potential Distribution in Mass Spectrometer Ion Sources

W. M. BRUBAKER
*Consolidated Engineering Corporation, Pasadena, California*
(Received October 11, 1954; revised manuscript received April 18, 1955)

The role of space charge as a factor influencing the potentials and potential gradients in a mass spectrometer ion source of the electron bombardment type is calculated. Planar equipotential surfaces are assumed, and the analysis then becomes that of a plane parallel positive ion diode. The "cathode" of the ion diode may be either emission-limited or space-charged-limited. The analysis considers the charge of the electrons in the ionizing sheet and the charge of the positive ions in the diode.

At a critical gas pressure the influences of the positive and negative charges on the potential of the ionizing region are equal and opposite, for small ionizing current. This concept leads to a pressure normalization in terms of the critical pressure. For a given source geometry and electron bombarding energy one can construct universal curves which give the potentials and the potential gradients as a function of the normalized gas pressure and the ratio of the ionizing electron current density to the repeller voltage. Experimental data are in agreement with the predictions of the theory.

## INTRODUCTION

An appreciation of the phenomena which occur in a mass spectrometer ion source of the electron bombardment type is obtained from an analysis of what happens to the potentials and the potential gradients in the source when space charge effects are present. In spite of the small dimensions of such ion sources and the minuteness of the electron and ion currents used, space charges grossly alter the potential (and gradient) distribution. Thus the early portions of the ion trajectories may be sensitively influenced by space charge.

In this work the potential and the potential gradient at the ionizing region are calculated, and the results are presented as a set of general curves using normalized variables. The analytical expressions indicate the influence of ionizing electron current, gas pressure and ionizing probability, and the ion repeller voltage for any combination of these independent variables. The explicit dependence of space charge phenomena on the design parameters of the source geometry is obtained.

For purposes of analysis the equipotential surfaces in the source are assumed to be parallel planes, and any influence of the ion accelerating gradient which "leaks" through the first slit is ignored. Where possible the variables are normalized so that the analysis is carried out in dimensionless numbers.

The knowledge of the actual potential of the ionizing regions, as given in this paper, is of particular importance to one who does appearance potential studies.

## GENERAL

The geometry of an idealized mass spectrometer ion source in which the equipotentials are assumed to be portions of parallel infinite planes is given in Fig. 1. The ionizing electron current is shown to flow in a sheet from the filament to the anode in the ionizing plane. Because the anode to which the electrons flow is of relatively small dimensions, it is shown as intercepting only a portion of the current in the large sheet.

The region between the ionizing plane and the first slit plane contains only positive ions, and constitutes a positive ion diode. The "cathode" of this diode is the ionizing plane, and the "anode" is the first slit plane. The gradient on the first slit side of the ionizing plane is frequently not zero, and in these instances the flow of current in the ion diode is emission-limited. The relation between the cathode gradient of an emission-limited plane-parallel diode and the current density is given in the literature.[1,2] The nomenclature and the results of reference 2 are used throughout this paper.

Typical potential distributions as functions of position between the repeller and the first slit plane are given in Fig. 2. In the absence of any space charge the voltage gradient in the source is uniform, and the potential distribution is given by curve 1. If an ionizing electron current $I_1$ is added at zero pressure (no positive ions) the electron space charge depresses the potentials as in curve 2. As we hold the ionizing current density constant and admit gas to the source in two consecutive steps the potentials rise as shown by curves 3 and 4. These potential distributions are based on the assumption that no negative ions are formed in the source.

In the course of this analysis it was discovered that it is extremely convenient to normalize the pressure in

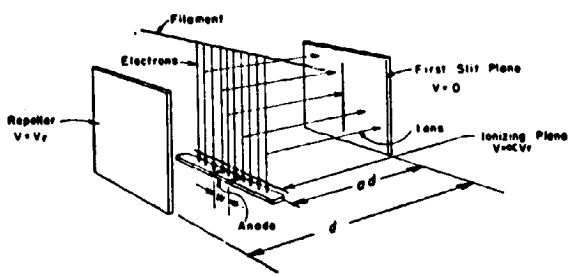


FIG. 1. Geometry of idealized ion source. The electron beam is constrained to the sheet by a magnetic field.

[1] H. F. Ivey, Phys. Rev. 76, 554 (1949).
[2] W. M. Brubaker, Phys. Rev. 83, 268 (1951).

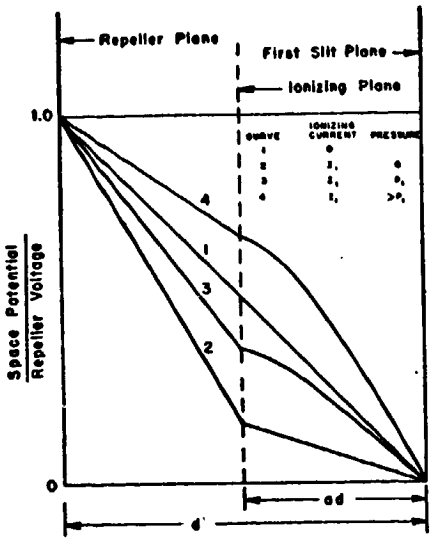


FIG. 2. Space potential *vs* position for typical conditions of operation. $I_1$ is an arbitrary value of ionizing electron current which is the same for curves 2, 3, and 4.

the source to that pressure at which, for the ionizing plane, the influence of the electron space charge in the ionizing sheet is exactly neutralized by the positive ion space charge at low ionizing currents. This pressure is noted as $P_c$, the critical pressure. A typical potential distribution at the critical pressure is shown in Fig. 3.

One of the main objectives is the calculation of the potential of the ionizing region as a function of the geometry, the ionizing current density, the pressure and the ionizing probability of the gas present in the source. This potential is normalized to the repeller potential by the dimensionless variable $\alpha$. When $\alpha$ is known, several other parameters such as the gradient at the ionizing sheet, the ion current density relative to the space-charge-limited ion current density for the same diode potentials, etc., are also known. The potential of any plane in the source can be calculated with the equations given in reference 2, if desired.

The analysis is divided logically into three regions of increasing ion currents which are assumed to be proportional to the product of the anode current and the pressure. The regions are characterized as follows.

## Region I

This region is bounded on the lower end by zero space charge, and on the upper end by the condition of space-charge-saturation (zero gradient) at the cathode of the positive ion diode. The single positive ion diode is emission-limited in this region.

## Region II

Zero gradient on the first slit side of the cathode of the positive ion diode and a finite gradient on the repeller side define this region. Thus we have a single space-charge-limited diode.

## Region III

At still higher ion currents the ions are formed at such a fast rate that they are not all drawn to the plane of the first slit. This happens when the potential of the ionizing sheet is equal to or greater than the repeller voltage. Thus the positive ion space charge causes the potential of the ionizing region to rise above that of the repeller, and we have zero gradient on both sides of the electron beam, or two space-charge-limited diodes in parallel.

The analysis of region I is made in two parts: one of a low current level, and one of a high current level. From the consideration of the low current level phenomena comes the concept of a "critical" pressure. This proves to be a most useful normalization which greatly aids the analysis at the high current levels.

The definitions of the symbols used are given in Table I. The variable $i_V$, the anode current in microamperes divided by the repeller voltage, is the only variable whose physical meaning is not obvious. It has the appearance of a transconductance, but the anode current and the repeller voltage are independent of each other. Their influence on the potentials in the source, however, is determined uniquely by their *ratio* independently of their individual magnitudes. This comes about because the influence of the electron beam is to depress the space potentials while the repeller voltage raises them.

In combination with the definitions of Table I, and the concept that the anode intercepts a portion of the electron current which flows in a sheet, $i_V$ is expressed as:

$$i_V=\frac{wj_{e1}\times 10^6}{V_r}, \tag{1}$$

$$i_V=\frac{w\sigma\times 10^6}{V_r}\left(\frac{2V_{e1}e}{m_e}\right)^{\frac{1}{2}}. \tag{2}$$

Any dependence of $V_{e1}$ on the potential of the ionizing region is neglected. A form of Poisson's equation in rationalized mks units states

$$\Delta(dV/ds)=\sigma/\epsilon_0, \tag{3}$$

where in our case $\Delta(dV/ds)$ is the difference in the gradient on the two sides of the ionizing plane, and $\sigma$ is the electron charge per square meter in the ionizing sheet.

The gradient on the first slit side of the ionizing plane is the cathode gradient of the positive ion diode. For emission-limited conditions the normalized density of ion current is related to the normalized cathode gradient by[2]

$$\rho=\tfrac{1}{2}+(\tfrac{1}{2}-\tfrac{3}{4}\gamma)(1+3\gamma)^{\frac{1}{2}}. \tag{4}$$

Combination of Eqs. (2) and (3) with the definition of

$\gamma$ leads to

$$i_V=\frac{1}{A}\left[(1-\alpha)-\frac{1-a}{a}\alpha\gamma\right], \tag{5}$$

where

$$A=\frac{(1-a)d\times10^{-6}}{\epsilon_0 w}\left(\frac{m_e}{2V_{el}e}\right)^{\frac{1}{2}}$$

and is a constant for a given source operated at constant electron energy.

The flow of positive ions through the diode, according to the Child-Langmuir equation and the definition of $\rho$ yields

$$j_{+\text{ion}}=\frac{4\rho}{9}\left(\frac{2e}{M}\right)^{\frac{1}{2}}\frac{(\alpha V_r)^{\frac{1}{2}}\epsilon_0}{(ad)^2}. \tag{6}$$

The physics of the ionization process gives us a relation between $j_{+\text{ion}}$ and $j_{el}$

$$j_{+\text{ion}}=\frac{SP_{\text{mm}}V_r i_V}{w}\times10^{-6}. \tag{7}$$

The Eqs. (4) through (7) give us sufficient information to allow us to eliminate any three of the four variables $\alpha$, $\gamma$, $\rho$, and $j_{+\text{ion}}$, and to express the remaining one as a function of $i_V$ and the source parameters $a$, $d$, $w$, and $V_{el}$ as given by $A$.

In region II the diode is space-charge-limited and so $\rho$ and $\gamma$ have the constant values of unity and zero, respectively. This greatly simplifies the equations.

### *Analysis, Region I*

*Low current solution.*—The first instance in which approximation for ease of manipulation can be made without loss of accuracy at low levels is in Eq. (4).

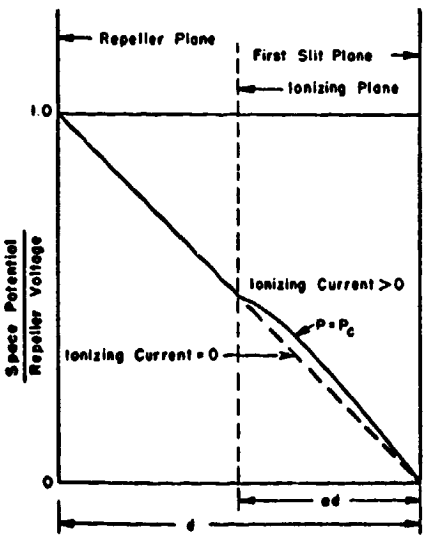


FIG. 3. Space potential *vs* position when $P$ is the critical pressure, $P_c$. ($x=1$.)

TABLE I.

$V_r$ = repeller voltage, volts, relative to the potential of the first slit plane, which is at $V=0$;

$\alpha V_r$ = potential of the ionizing plane;

$V_{el}$ = energy of ionizing electrons, electron volts;

$d$ = depth of ion source, repeller to first slit, meters;

$ad$ = distance from ionizing region to the first slit, meters;

$e$ = electronic charge, $1.6\times10^{-19}$ coulombs;

$j_{el}$ = electron current per meter in ionizing sheet;

$M$ = mass of positive ion, kilograms;

$m_e$ = mass of electron, $9\times10^{-31}$ kilograms;

$j_{+\text{ion}}$ = ion current density, amperes/sq meter;

$$i_V=\frac{\text{anode current in microamperes}}{\text{repeller voltage, volts}};$$

$$\gamma=\frac{\text{gradient at the cathode of the positive ion diode in the presence of positive ion space charge}}{\text{gradient at the cathode of the positive ion diode in the absence of positive ion space charge, at the same } \alpha};$$

$$\rho=\frac{\text{actual positive ion current density}}{\text{space-charge-limited positive ion current density, at the same } \alpha};$$

$\epsilon_0$ = permittivity of free space, $8.85\times10^{-12}$ farads/meter;

$S$ = number of ion pairs formed per electron per meter of electron path at 1 mm Hg pressure;

$$x=\frac{\text{pressure, mm Hg}}{P_c\text{, the critical pressure, mm Hg}}=\frac{P_{\text{mm}}}{P_c};$$

$w$ = width of ionizing electron sheet intercepted by the anode, meters.

For $\rho$ small (4) becomes

$$\gamma\doteq1-\frac{16}{27}\rho. \tag{4a}$$

If we use Eqs. (4a), (5), (6), and (7) to eliminate $\rho$, $j_{+\text{ion}}$ and $\gamma$ from Eq. (5), we obtain

$$\alpha^{\frac{1}{2}}+a\alpha^{\frac{1}{2}}[Ai_V-1]=\tfrac{1}{2}a^2dSP_{\text{mm}}\left(\frac{MV_{el}}{m_eV_r}\right)^{\frac{1}{2}}Ai_V. \tag{8}$$

Equation (8) is readily solved for the conditions of small $i_V$ by letting

$$\alpha=a(1+2\delta). \tag{9}$$

When Eq. (9) is set into Eq. (8).

$$\delta\doteq\frac{A}{2}\left[\tfrac{1}{2}dSP_{\text{mm}}\left(\frac{aV_{el}M}{V_rm_e}\right)^{\frac{1}{2}}-1\right]i_V. \tag{10}$$

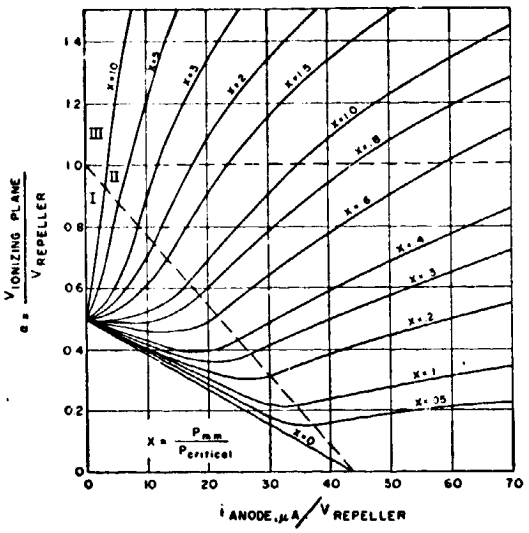


FIG. 4. Potential of the ionizing region as a function of $i_V$. regions I, II, and III are separated by the two dotted straight lines. The regions are characterized as: region I—one emission-limited diode; region II—one space-charge-limited diode; and region III—two space-charge-limited diodes in parallel.

Equation (10) is entirely satisfactory for the rate of change of $\delta$ (or $\alpha$) with respect to $i_V$ as $i_V \rightarrow 0$. It also shows the possibility of having the potential of the ionizing region independent of $i_V$. The pressure at which this occurs we shall call the critical pressure, $P_c$. It is given by

$$P_c = 3(V_r m_e / a V_{e1} M)^{\frac{1}{2}} / 4dS, \tag{11}$$

and if we define $x$ by the equation

$$P_{mm} = xP_c \tag{12}$$

Eq. (10) becomes

$$\delta \doteqdot (x-1)Ai_V/2 \tag{13}$$

and Eq. (9) becomes

$$\alpha \doteqdot a[1+A(x-1)i_V]. \tag{14}$$

For $i_V$ small this is an excellent approximation.

The approximate solution as represented in Eqs. (13) and (14) is sufficiently accurate for many of the operating conditions found in actual practice. However, it is not applicable in all cases, and so it is expedient to consider the phenomenon without the approximations.

*Large current solution.*—If we combine Eq. (11) for the critical pressure with the Eqs. (4) through (7) we can calculate the potential variations and display the results for any given source in a set of curves in normalized variables. A combination of Eqs. (5), (6), (7), (11), and (12) yields

$$\frac{1+\frac{1-a}{a}\gamma}{\rho^{\frac{1}{2}}} = \frac{4}{9a}\left[\frac{2(1-a)}{A}\right]^{\frac{1}{2}}(i_V^{-\frac{1}{2}} - Ai_V^{\frac{1}{2}})\frac{1}{x^{\frac{1}{2}}} \tag{15}$$

or

$$F(\gamma,\rho) = x^{-\frac{1}{2}}G(i_V). \tag{16}$$

The explicit form of Eq. (16) is too complicated for direct computation. However, $F(\gamma,\rho)$ can be plotted as a function of either $\gamma$ or $\rho$ for a given source. Similarly, $G(i_V)$ can be plotted as a function of $i_V$. Then, using $x$ as a parameter, families of curves can be obtained relating $\gamma$ and $\rho$ to $i_V$. Further, $\alpha$ as a function of $i_V$ can be obtained from $\gamma$ through the use of Eq. (5).

### *Analysis, Region II*

In region II the positive ion current flows across the diode under space-charge-limited conditions at the ionizing sheet. The relation between the ion current density and the voltage across the diode is given by the Child-Langmuir equation

$$j_{+\text{ion}} = \frac{4}{9}\left(\frac{2e}{M}\right)^{\frac{1}{2}}\frac{(\alpha V_r)^{\frac{1}{2}}}{(ad)^2}\epsilon_0.$$

As the rate of ion production is uniquely determined by the anode current (of ionizing electrons), the ionizing probability, and the pressure of the gas in the source, it is the independent variable and the voltage the dependent variable. Thus, we can state

$$\alpha_{\text{region II}} = \alpha_{\text{boundary regions I and II}} \times \left(\frac{i_{V\text{region II}}}{i_{V\text{boundary regions I and II}}}\right)^{\frac{1}{2}}. \tag{17}$$

### *Analysis, Region III*

In region III $\alpha$ is greater than unity. Thus, ions flow in both directions from the ionizing region as space-charge-limited current. Again, the rate of production of the ions is assumed to be entirely independent of the potential of the ionizing region. The potential of the region adjusts itself so that the sum of the two diode currents is equal to the rate of ion production.

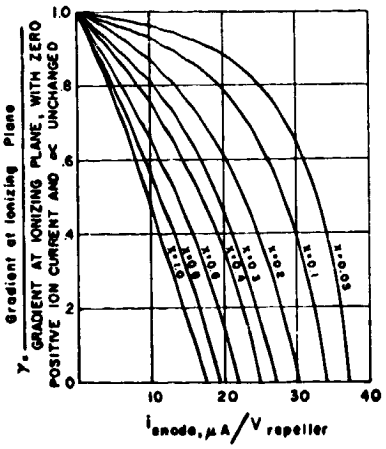


FIG. 5. Potential gradient at the ionizing plane as a function of $i_V$. The normalization is to the positive ion diode variables.

If we denote the ion current density to the first slit plane as $j_1$, and that to the repeller as $j_2$, we have

$$j_1=\frac{4}{9}\left(\frac{2e}{M}\right)^{\frac{1}{2}}(\alpha V_r)^{\frac{1}{2}}\epsilon_0/(ad)^2 \tag{18}$$

$$j_2=\frac{4}{9}\left(\frac{2e}{M}\right)^{\frac{1}{2}}[(\alpha-1)V_r]^{\frac{1}{2}}\epsilon_0/[(1-a)d]^2 \tag{19}$$

and

$$j_1+j_2=SP_{mm}j_{el}=\frac{4\left(\frac{2e}{M}\right)^{\frac{1}{2}}V_r^{\frac{1}{2}}\epsilon_0}{9d^2}\left[\frac{\alpha^{\frac{1}{2}}}{a^2}+\frac{(\alpha-1)^{\frac{1}{2}}}{(1-a)^2}\right]. \tag{20}$$

If we normalize the pressure as by Eqs. (11) and (12) this becomes

$$i_V=\frac{16\epsilon_0 w\times 10^6}{27xd}\left(\frac{2aeV_{el}}{m_e}\right)^{\frac{1}{2}}\left[\frac{\alpha^{\frac{1}{2}}}{a^2}+\frac{(\alpha-1)^{\frac{1}{2}}}{(1-a)^2}\right] \tag{21}$$

$$=B[\alpha^{\frac{1}{2}}+C(\alpha-1)^{\frac{1}{2}}]/x \tag{22}$$

where $B$ and $C$ are constants for a given source operated at constant electron ionizing energy.

## APPLICATION OF THE THEORY

A set of universal curves has been made for a typical ion source of the electron bombardment type. The data for the source are given as follows: $a=0.5$, $d=0.1$ inch $=2.54\times10^{-3}$ meter, $w=0.05$ inch $=1.2\times10^{-3}$ meter, and $V_{el}=70$ volts.

The dependence of the potential of the ionizing plane upon $i_V$ is shown in Fig. 4. The three regions are separated by the dotted straight lines. It is interesting to note that at low pressures the boundary between regions I and II is reached essentially as a result

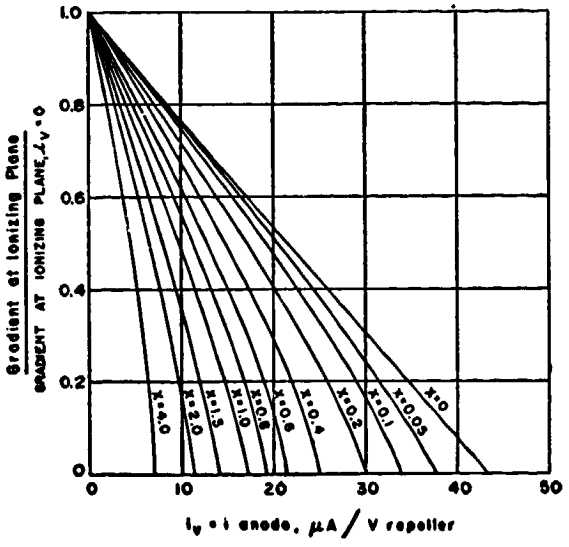


FIG. 6. Potential gradient at the ionizing plane as a function of $i_V$, normalized to the gradient when $i_V=0$.

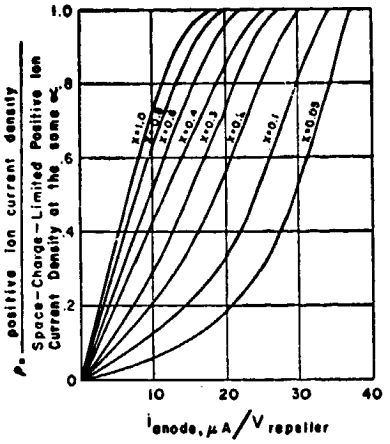


FIG. 7. Space-charge-saturation of positive ion current as a function of $i_V$, normalized to positive ion diode variables.

of the space charge of the electrons which lowers the potential across the positive ion diode to very low levels. At pressures above $x=1$ the potential of the ionizing region always increases with $i_V$, and at the higher pressures the potential of the ionizing region rises quite rapidly with $i_V$.

The normalized gradient on the first slit side of the ionizing region is shown in Fig. 5. $\gamma$ is defined in terms of the positive ion diode variables. Thus the gradient to which the data of Fig. 5 are normalized is the gradient which would exist if the potential of the ionizing region remained constant while the pressure was reduced to zero.

Because the normalization of $\gamma$ is to a gradient which is not experimentally realizable, it is interesting to plot the actual gradient normalized to its value at $i_V=0$. To do this we multiply by $\alpha/a$. This is done in Fig. 6. Here we see the influence of space charge on the gradient at the ionizing plane. It is obvious that this gradient is decreased by both the electron and the ionic space charges.

The normalized positive ion current density, $\rho$, as a function of $i_V$, is given in Fig. 7. Here again we see that at low pressures space-charge-limited conditions are reached primarily because the electron space charge lowers the diode voltage. At the higher pressures the rate of approach to space-charge-limited conditions is slowed by an increase of the diode voltage caused by the positive ion space charge. The normalization is in terms of the diode variables.

## EVALUATION OF THE APPROXIMATIONS

In order to facilitate a mathematical statement of the problem, two simplifying assumptions were made: (A) All equipotentials are parallel planes; and (B) the ionizing sheet of electrons is of infinitesimal thickness.

Neither of these is realized in practice. Assumption (A) makes the greater departure from reality, as the dimension of the electron beam in the direction parallel

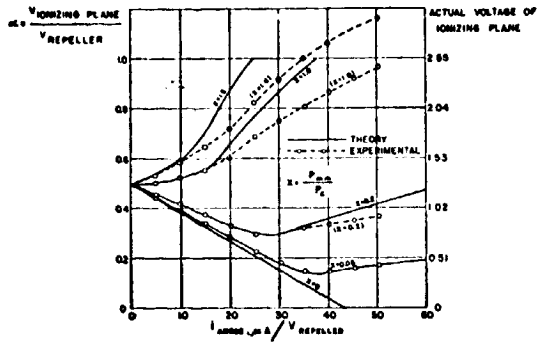


FIG. 8. Comparison of theory and experiment. The anode current was empirically adjusted to fit the low pressure curve, $x=0.05$. Remaining data were then plotted without further adjustment.

to the repeller plane is quite small. This causes the capacity of the ionizing region to be much greater than it otherwise would be. In addition the warping of the equipotentials in the vicinity of the space charge may be expected to have an important influence on the optical properties of the source. This may well be the mechanism of the influence of the presence of a second gas on the sensitivity of the instrument to a first gas.

Assumption (B) is of lesser importance. The influence of space charge on potentials outside the volume in which the charges reside is essentially a function of the total charge involved and independent of the distribution of the charges. Thus outside the ionizing region itself the potentials are relatively unaffected by the thickness of the electron beam. This paper ignores the distribution of potentials and gradients within the ionizing sheet, but it is felt that the conclusions drawn are little influenced by the distribution of electron current in the direction perpendicular to the plane of ionization.

## EXPERIMENTAL VERIFICATION OF THE THEORY

The soundness of the analysis is supported by experimental data which relates the potential of the ionizing region with anode current, repeller voltage, and the pressure. The data shown in Fig. 8 were taken by observing the change in ion accelerating voltage required to keep the ion beam on the collector of the mass spectrometer as the anode current and the pressure were varied. The actual potentials of the ionizing region are given as well as the relative values in terms of $\alpha$.

The anode current as plotted was normalized to fit the theoretical curve at the lowest pressure, and then the rest of the data were taken without further normalization. This empirical normalization is required because the electron beam is not in the form of a very broad (infinite) sheet, as was assumed for purposes of calculation. The capacity per unit area of the ionizing sheet is greater because of its finite size.

Since the influence of the electron space charge on the potential of the ionizing region varies inversely as the electrostatic capacity of the beam to its environs, we would expect the dependence of the space potential on the electron beam to be less than that calculated for infinite sheets. The same argument applies to the ions. In Fig. 8 the actual anode currents have been reduced by an arbitrary factor of 1.65 to obtain the degree of agreement shown between experiment and theory.

## CONCLUSIONS

The essential characteristics of the potentials and gradients in a mass spectrometer ion source are derived by treating the ion accelerating region as an emission-limited or space-charge-limited diode as the conditions require. A comparison of the theory with experimental data shows that the theory is correct in its essentials. When allowance is made for the increased capacity of the ionizing region owing to its finite size, the agreement between experiment and theory is satisfactory.

The knowledge of the dependence of the source potentials on the source variables (ionizing current, repeller voltage, pressure, etc.) is vital for appearance potential investigations. It is also necessary for an understanding of the influence of space charge on the optical properties of the source.

## ACKNOWLEDGMENTS

It is a pleasure to acknowledge the benefit of discussing this problem with Dr. Clifford Berry, Dr. Harold W. Washburn, and Mr. Lawrence Hall. Mr. Hall also obtained the experimental data.

## APPENDIX II

Abstract of a Paper Presented
at
Seventeenth Annual Conference on Mass Spectrometry
and Allied Topics

Operation of Quadrupole Mass Filter at High Pressure,*
W. M. Brubaker and W. S. Chamberlin, Earth Sciences, A Teledyne Company, Pasadena, California 91107.

An experimental investigation has been made of the operation of a quadrupole mass spectrometer in a high ambient pressure of hydrogen. Experiments with potassium ions from a Wolfram filament loaded with KCl indicated no observable deterioration in the resolving power at hydrogen pressures to $10^{-2}$ torr. Transmission efficiency of the ions through the 10-inch quadrupole is unchanged at hydrogen pressures to $5 \times 10^{-4}$ torr. At pressures above $3 \times 10^{-3}$ torr the transmission falls, reaching twenty percent at $10^{-2}$ torr. Experiments with the mercury spectrum, using an electron bombardment type ion source, show a somewhat increased deterioration of the performance as the pressure of hydrogen is raised. At pressures above $5 \times 10^{-5}$ torr the resolving power of the instrument begins to be decreased. At $5 \times 10^{-4}$ torr the resolving power at a given sensitivity is reduced about forty percent. A simple Faraday Cup collector electrode responds to a background current which is unrelated to the transport of ions through the quadrupole. This current is proportional to the ion production rate (ionizing electron current x pressure of hydrogen). It is independent of the rate of ion emission from the source and of the quadrupole excitation potentials. These data suggest that the background signal is caused by photons emitted by excited hydrogen molecules.

---

* This research was supported in part by the National Aeronautics and Space Administration under contract No. NASW-1736.

END

DATE

FILMED

SEP 18 1969